Title

I. LATTICE HEAT CAPACITIES OF ALLOYS AT LOW TEMPERATURES; InPb, AuCd, Mg3Sb2. II. EFFECT OF ORDERING ON LATTICE HEAT CAPACITY; AuCu3

Author

Yoon, Hong Il.

Publication Date

1971-08-01

I. LATTICE HEAT CAPACITIES OF ALLOYS AT LOW TEMPERATURES; InPb, AuCd, Mg_3Sb_2

II. EFFECT OF ORDERING ON LATTICE HEAT CAPACITY; $AuCu_3$

Hong Il Yoon

(Ph.D. Thesis)

August, 1971

AEC Contract No. W-7405-eng-48

DISCLAIMER

LBL-101

I. LATTICE HEAT CAPACITIES OF ALLOYS AT LOW TEMPERATURES; InPb, AuCd, Mg_3Sb_2

II. EFFECT OF ORDERING ON LATTICE HEAT CAPACITY; $AuCu_3$

Hong Il Yoon

(Ph. D. Thesis)

August, 1971

UNIVERSITY OF CALIFORNIA

Lawrence Berkeley Laboratory
Berkeley, California

AEC Contract No. W-7405-eng-48

I. LATTICE HEAT CAPACITIES OF ALLOYS AT LOW TEMPERATURES; InPb, AuCd, Mg_3Sb_2

II. EFFECT OF ORDERING ON LATTICE HEAT CAPACITY; $AuCu_3$

Hong Il Yoon

Inorganic Materials Research Division
Lawrence Berkeley Laboratory
and
Department of Materials Science and Engineering
College of Engineering
University of California
Berkeley, California

August, 1971

ABSTRACTS

Part 1.

Heat capacities of three alloys were measured by isothermal calorimetry from 20° to 298°K. The alloys were InPb, endothermically formed from the elements, the moderately exothermic AuCd, and the highly exothermic Mg_3Sb_2. Deviations from Kopp's law of additivity of C_p were rather small, except for a small anomaly of undetermined origin at 240° to 300°K for InPb, and a decided negative deviation (~5%) above 200°K for Mg_3Sb_2.

InPb deviates positively from Kopp's law below 100°K; the maximum deviation at 30°K amounts to 0.3 cal/g-atom deg.

Above 100°K, it deviates negatively up to about 0.1 cal/g-atom deg. just below the anomaly, where it becomes positive. The integrated $\Delta H_{st} - \Delta H_0$ and $\Delta S_{st} - \Delta S_0$ amount to -1 cal/g-atom and 0.464 eu, respectively. The total heat of the anomaly is about 14 cal/g-atom; the entropy, about 0.03 eu. AuCd deviated negatively from Kopp's law below 200°K, trending to positive at higher temperatures, the maximum deviation being about 0.1 cal/g-atom deg. Integrated effects were -14 cal/g-atom for $\Delta H_{st} - \Delta H_0$ and -0.027 eu for $\Delta S_{st} - \Delta S_0$. Mg_3Sb_2 had positive deviations below 70°K, trending to negative nearly 0.3 cal/g-atom deg. above this temperature. Integrated effects were -50 cal/g-atom for $\Delta H_{st} - \Delta H_0$ and -0.072 eu for $\Delta S_{st} - \Delta S_0$.

Part 2.

Heat capacities of the $AuCu_3$ alloy in both the ordered and disoredered states have been measured between 20° and 298°K by isothermal calorimetry. Combining the heat capacity data for $AuCu_3$ from this study with existing high temperature thermodynamic data, $S^\circ_{0,\text{disordered}}$, the configurational entropy, was found to be 0.987 eu, which is somewhat lower than the theoretical value for complete disorder, 1.117 eu. The difference may be explained in terms of short-range order, the

existence of which is confirmed by heat of formation measurements with tin solution calorimetry.

The heat capacities of both states show small positive deviations from the Kopp's law value up to 170°K above this temperature the deviations become slightly negative. However, the heat capacity of the disordered state is slightly higher than that of the ordered state below 130°K by a maximum amount of 0.06 cal/g-atom-deg. at 70°K. From 130°K to room temperature the difference is practically zero. In agreement with previous Debye temperature measurements on $AuCu_3$ at helium temperatures (below 4.2°K), a small but definite decrease of C_p on ordering was observed.

I. INTRODUCTION

It is of great interest to know how alloying affects the vibrational heat capacity and whether bond strength is related to lattice heat capacity. It would be a reasonable hypothesis that ΔC_p (heat capacity difference between the alloy and its components) is positive for endothermic alloys, because bonding is looser than in the elements and a higher Debye temperature might be expected. The opposite hypothesis would be reasonable for exothermic alloys.

Few studies have been made on this problem. In the compilation by Hultgren, Orr, Anderson, and Kelley in 1963[1] and theri supplementary work to date[2] 288 systems have been evaluated. Of these systems, for only seven substitutional nonmagnetic alloys has C_p been measured at temperatures between 20° and 298°K where lattice heat capacity should show effects.

Most low temperature C_p studies of alloys have been made in the liquid helium range (below 4.2°K) for the special purpose of determining the electronic heat capacity. Knowledge of electronic heat capacity is of great interest in obtaining an understanding of the density of states of the Fermi electron gas in the metallic state. These measurements do not clearly show, however, the effect of alloying on the vibrational (Debye) heat

capacity. Although direct measurements are not plentiful, some conclusion should be possible from entropies of formation, where they have been measured

$$\Delta S_T = \Delta S_0 + \int_0^T \frac{\Delta C_p \, dT}{T} \quad .$$

Since, by the third law, S_0 is zero for the elements, the entropy of formation at zero, ΔS_0, is simply the configurational entropy. Hence, deviations from the configurational entropy of formation are dictated by the integrated sign of ΔC_p. A clue to a relationship between ΔH and ΔC_p such as proposed in the first paragraph might be found by examining the relationship between ΔH and ΔS.

Anderson[3] sought such a relationship at 50 atomic percent compositions for 45 liquid alloys for which he felt the entropies of formation were reasonably well known. Since these should have nearly ideal configurational entropies, ΔS^{xs} was compared with ΔH. Of course, other factors contribute to ΔC_p, and hence to ΔS^{xs}, besides the vibrational term which we are considering. For example, there is the electronic contribution, the dilation contribution, $(C_p - C_v)$, and various anomalous effects such as magnetic transformations. So we cannot expect precise relations, but might find statistically that there are definite trends. As can be seen in Fig. 1, there is a decided trend. Of 25 exothermic systems of Anderson's study, only two had a positive

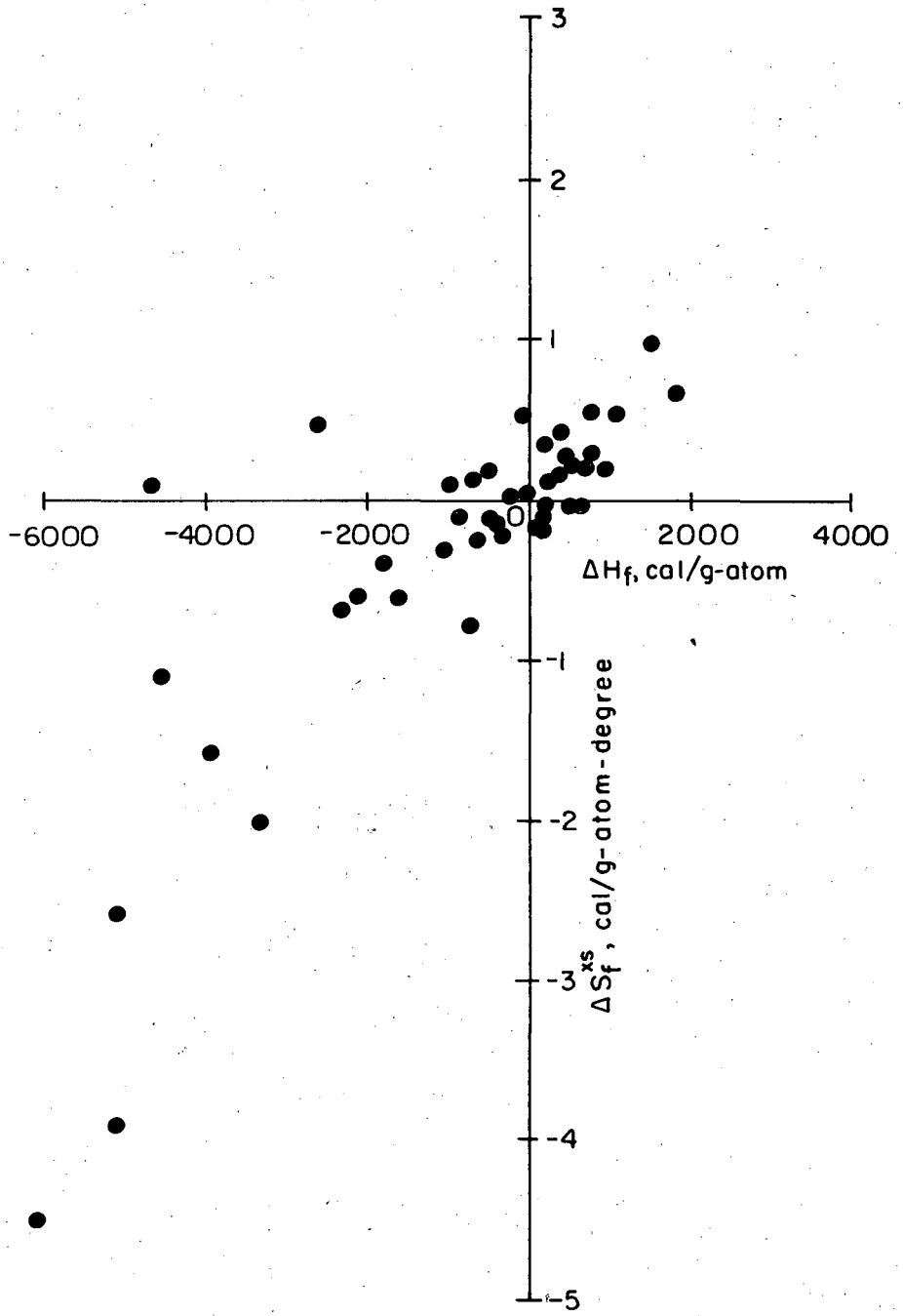

FIG. 1 ΔS_f^{xs} VERSUS ΔH IN LIQUID EQUIATOMIC SOLUTIONS

XBL 716-6899

ΔS^{xs}, eight were zero within experimental error, and 15 had negative values for ΔS^{xs}. Of 20 endothermic systems, only two had a negative ΔS^{xs}, six were near zero, and 12 had positive values of ΔS^{xs}.

For solid alloys the configurational entropies may vary widdly. 39 ordered solid alloys which should be without magnetic anomalies were examined in this study. For these, since the configurational entropies should be near zero, ΔH was compared with ΔS with the results shown in Fig. 2. Here also there is a statistical correlation, though the center of the curve is displaced toward negative values of ΔH. The correlation would closely resemble Fig. 1 if ΔH were plotted against ΔS^{xs}. The reason for this was not understood.

The heat of formation, ΔH, represents the energy of bonding in the alloy minus the energy of bonding in the component pure elements. Exothermic alloys should have tighter bonds, higher vibrational frequencies, and lower C_p values at low temperatures than the average of the elements; hence, ΔC_p should be negative for the vibrational contribution to C_p. Conversely, endothermic alloys should behave oppositely.

The quasi-chemical model[4] explains the relationship between enthalpy of formation and bonding energy in the simplest way. This model clearly has shortcomings. However, it

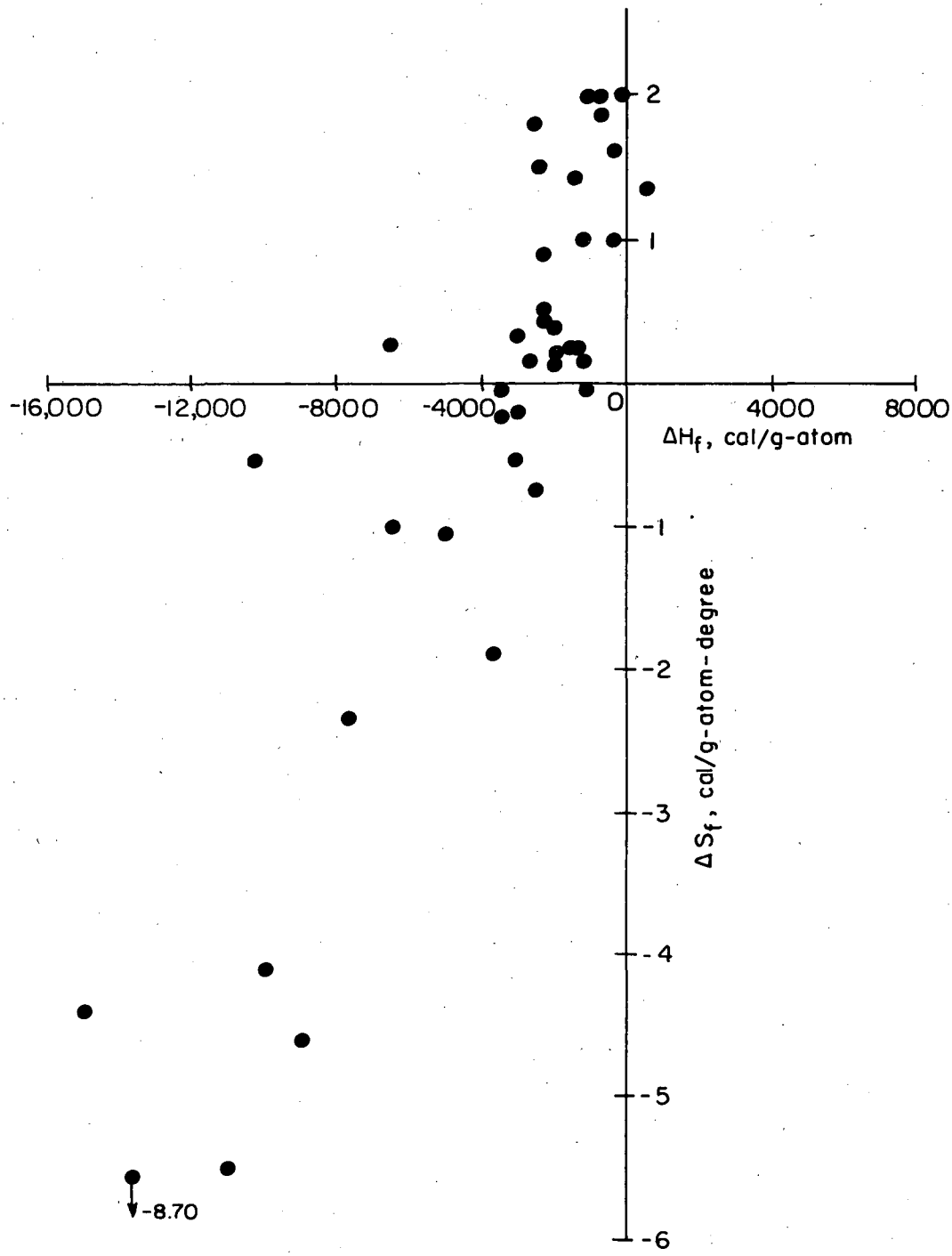

FIG. 2 ΔS_f VERSUS ΔH_f IN SOLID ORDERED ALLOYS

XBL 716-6900

qualitatively explains many facts. In this model the energy of a phase equals the sum of the energies of bonds between nearest neighbors. The bond energies are supposed to be the same at all compositions; no provision is made for such factors as geometric strain when atoms differ in size; interactions between more distant atoms are also not considered. Consider a phase containing x mole fraction of A atoms and y mole fraction of B atoms to form the A_xB_y alloy. Then the heat of mixing (ΔH_m) could be expressed as follows:

$$\Delta H_m = H_{alloy} - (xH_A + yH_B).$$

The first order approximation (random mixing) gives ΔH_m in terms of bonding energy between atoms as follows:

$$\Delta H_m = -P_{AB}\left[H_{AB} - \tfrac{1}{2}(H_{AA} + H_{BB})\right]$$

where P_{AB} is the number of bonds of type A-B

and H_{AB}, H_{AA}, and H_{BB} are the bonding energies between the atoms.

The above equation shows that if the bonding energy between dissimilar atoms is larger (more attractive) than the average bonding energy between similar atoms, the system will be exothermic. Likewise, the heat of formation is positive if the bonding energy between dissimilar atoms is smaller (more repulsive) that the average bonding energy.

The main contribution to heat capacity comes from lattice vibrations and electronic excitations if no transformations occur in the pertinent temperature range. The electronic term is the most importnat when temperature is so low that the lattice term becomes small. This electronic term becomes larger in absolute value at elevated temperatures, but not so fast as the lattice term. The lattice heat capacity is the principal term at temperatures above ~20°K. Einstein showed the influence of quantum effects on C_p and Debye derived an expression agreeing better with experiments. The Debye expression assumes a broad spectrum of lattice vibrational frequencies with a maximum cut-off frequency. It shows C_p should be proportional to T^3 at very low temperatures. The classical Debye equation for the lattice heat capacity of crystals can be expressed as

$$C_v \simeq C_p = \int_0^{\mu_D} g(\mu)\,(h\mu/kT)^2 \frac{ke^{h\mu/kT}}{\left(e^{h\mu/kT}-1\right)^2}\,d\mu$$

where $g(\mu) = a\mu^2$ is the density of states and μ_D is the maximum cut-off frequency.

It must be noticed that the simplified Debye elastic continuum model considers identical atoms in isotropic crystals. For pure metals, measurements of low temperature elastic constants furnish a means of determining the maximum Debye frequency.

In alloys, $g(\mu)$ functions are not so simple as they are for pure metals, making it difficult to modify the classical Debye equation for the calculation of heat capacities of alloys. Furthermore, the low temperature elastic constants of alloys are usually not available. While quantitative predictions of heat capacities of alloys cannot be made from the Debye theory, the classical model of bond energy theory qualitatively suggests that heat capacity should decrease with increasing bond strength as judged from ΔH. From the simple harmonic model of atomic vibration, the vibrational frequency is proportional to the elastic constants of the material as the following equation indicates,[5]

$$\mu = 1/2\pi\sqrt{ya/m}$$

where a = lattice constant

m = mass of atom

y = elastic constant.

The Debye temperature is related to the Debye frequency as follows:

$$\theta_D = h\mu_D/k$$

where h = Planck's constant

k = Boltzmann constant.

As may be seen from the above two equations, the stronger bond (judged from the larger elastic constant) should have a higher vibrational frequency, and therefore a higher Debye temperature and a lower heat capacity.

Magnetic contributions, phase changes, and other effects that cause anomalies in C_p might have large thermal entropy contributions; this could reverse the predicted relations of ΔC_p and ΔS.

Usually Kopp's law suffices to estimate C_p values reasonably satisfactorily at high temperatures. Nevertheless, the deviation from Kopp's law can vary appreciably at low temperatures where C_p is changing rapidly. From the equation

$$S_{vib.} = \int_0^T \frac{C_{p(vib.)}}{T} dT ,$$

it can be seen that low temperature heat capacity is particularly important to the entropy since temperature is in the denominator. The scarcity of low temperature heat capacity measurements of alloys make it difficult to test the validity of the above mentioned correlations.

The purpose of the present study was to investigate the relationship between ΔH_f and ΔC_p experimentally.

The seven systems mentioned on page 1 which have low temperature heat capacity measurements are: AlSb,[6] InSb,[6,7] Mg_2Sn,[8] LiMg,[9] Cd-Mg,[10,11] AuCu,[12] and Cu-Zn.[13] They are all exothermic systems and show negative deviations from Kopp's law.

Three systems with large differences in heats of formation were chosen for this study. These are InPb, AuCd, and Mg_3Sb_2 alloys, whose heats of formation range from positive to highly negative.

Th InPb system has a positive enthalpy of formation at room temperature in the solid state. Measurements by liquid tin solution calorimetry[14] at 315°K showed the heat of formation of the alloy to be 300 cal/g-atom. From differential-thermal-analysis measurements, Heumann and Predel[15] reported ΔH to be 400 cal/g-atom at this composition. Lead has a face-centered-cubic structure isotypic with copper. Indium has the same structure except that the c-axis is elongated by about 7.6%, making its symmetry face-centered tetragonal. The equiatomic composition of the InPb system was chosen because this composition has the maximum endothermic heat of formation in the alloy. The melting point of the alloy of this composition is about 510°K.

The AuCd (β-phase) alloy has a relatively large negative heat of formation (-4500 cal/g-atom). It melts nearly congruently at 900°K. The phase region of the β-phase is not well determined and the structure at room temperature also is not well known.[16,17] At elevated temperatures the ordered CsCl (B2) structure exists,

with a = 3.312 Å at 50.1 atomic % of Cd. Two different diffusionless transformations have been found in cooling different compositions of this phase.[17] At about 50 atomic % Cd, a tetragonal structure was found at 30°C, whereas an orthorhombic structure was found at 60°C in alloys with 47.5% Cd.[17] The structures of the transformed phases are not well established. The selected value of the heat of formation of the β-phase is -4610 cal/g-atom at the 50-50 composition, based on the work of Kleppa[18] and Kubaschewski.[19]

The Mg_3Sb_2 alloy has the largest exothermic heat of formation of systems studied. The melting point of stoichiometric Mg_3Sb_2 is reported to be 1518°±5°K which is very much higher than those of Mg (923°K) and Sb (903°K). It exists in two polymorphic forms: α-Mg_3Sb_2, which has the tetragonal ($D5_2$) structure isotypic with La_2O_3 with a = 4.582 Å and c = 7.423 Å, and which transfroms above about 1180° ± 20°K to β-Mg_3Sb_2 which has the ($D5_3$) structure isotypic with Mn_2O_3. The range of existence of neigher α-nor β-Mg_3Sb_2 has been determined. ΔH_m = -15300 (±2000) cal/g-atom at 800°K, was taken from measurements by Kubaschewski and Walter,[20] as revised by Kubaschewski and Catterall.[21]

The method used to measure the C_p values in this study was isothermal calorimetery. Isothermal calorimeters were first

used by Eucken[22] and Nernst[23] and further developed by Giauque and his coworkers;[24,25] the calorimeter used in this work was patterned after Giauque's design, first built by Huffstutler[13] and rebuilt by Hawkins.[26] From measurements of the energy input, determined from the heater voltage and current, and the temperature rise of the calorimeter as measured by a resistance thermometer, the heat capacity was determined by dividing the energy input by the temperature rise.

II. EXPERIMENTAL

A. Calorimeter

The calorimeter consists of a specimen container (made of copper) around which a fine gold wire is wound. This gold wire serves both as a heater and resistance thermometer. The calorimeter can is surrounded by a heavy jacket (large copper block with large lead mass on the top) to provide large heat capacity and good conductivity of the jacket. The entire calorimeter-jacket assembly is surrounded by a Monel can soft soldered with 60/40 solder to the top supporting plate. This whole assembly is contained in a long steel container with a glass Dewar inside to hold a cooling medium like liquid hydrogen, liquid nitrogen, or dry ice-acetone. Figure 3 shows the general arrangement of the apparatus. Complete details of the calorimeter are given in Hawkins' dissertation.[26]

B. Measurement

Liquid hydrogen (between 20°-78°K), liquid nitrogen (78°-196°K), and dry ice with acetone (196°-300°K) were used as cooling media. Sometimes ice-water was used between the ice point and room temperature or between 250°-300°K to keep the drift rate down. As much sample as possible was packed into the calorimeter in

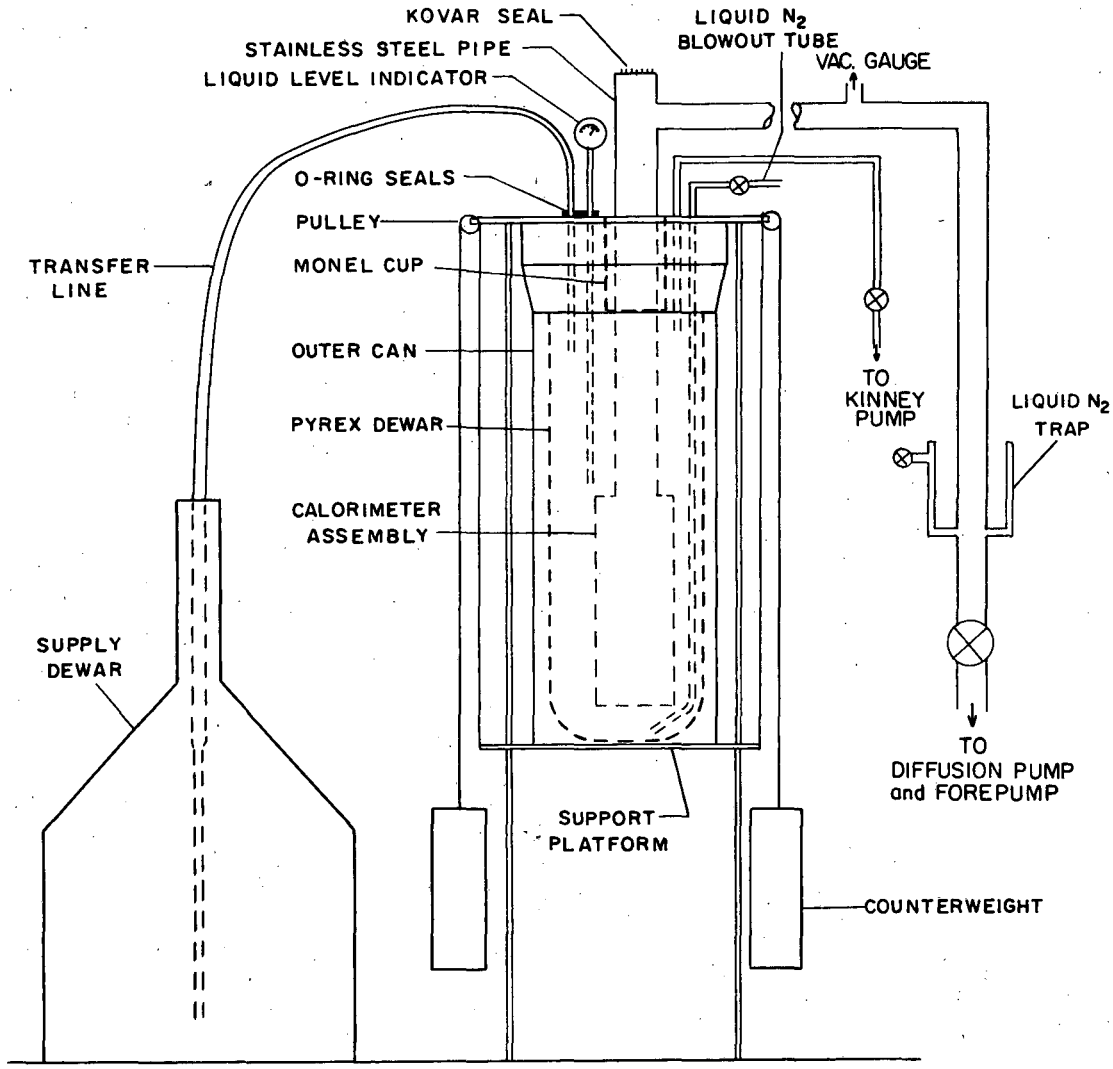

FIGURE 3 GENERAL ARRANGEMENT OF APPARATUS.

XBL 6912-6633

rod shape or in powder shape in case the sample is poorly conductive. Helium gas was introduced into the calorimeter can through a pin hole on the top of the calorimeter after filling with sample. After the vessel was evacuated in a dessicater and filled with an atmosphere of helium gas, the pin hole was selaed with soft solder. The calorimeter was left in the dessicater for 30 to 60 minutes to remove possible moisture. Then the whole calorimeter with sample was weighed. No change of weight after 24 hours indicates a tight seal. Increase of the weight would be due to leakage of air replacing helium gas. At low temperatures (mostly in liquid hydrogen runs) where the heat capacity changes rapidly, the energy input was adjusted so that the temperature rise of the calorimeter was of the order of 1degree during a single measurement. At higher temperatures the temperature rise was gradually increased to 4 degrees. The length of time for a measurement was about 7 to 9 minutes. During the heating time, measurements were made of heater current I_H and heater voltage E_H at one minute intervals. The jacket temperature was only approximately constant usually drifting a few hundreds of a degree during the measurements. This difference was read from the jacket thermocouple and corrected in the calculation. The time-temperature distribution for a typical run is shown in Fig. 4.

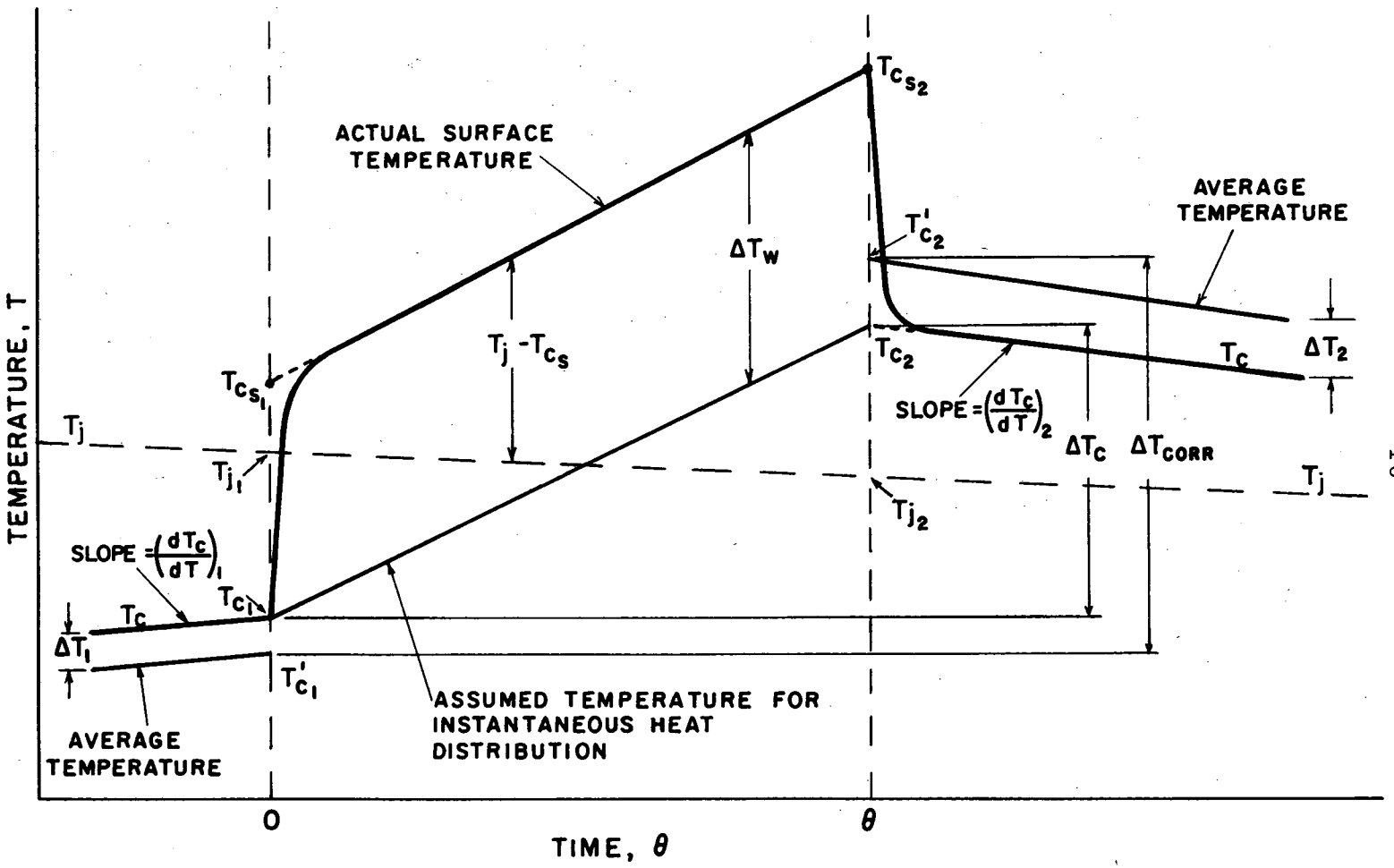

FIGURE 4. TIME-TEMPERATURE DISTRIBUTION FOR A TYPICAL RUN.

XBL 6912-6635

The total energy input was calculated as $\mathcal{E} = \tilde{E}_H \cdot \tilde{I}_H \cdot \theta$, where θ is the heating time, and $\tilde{E}_H$ and $\tilde{I}_H$ are average values obtained at 0.21θ and 0.79θ.

Corrections to both the energy and temperature rise were small (less than 5%) and arose from the following sources:

(1) heat leaks along the wires and supports

(2) radiation heat transfer due to temperature differences between the jacket and the calorimeter.

(3) temperature gradients in the sample during heating because the heating wire was wound around the outside of the can.

The final form of the energy input and corrected temperature rise of the calorimeter are as follows:

$$\Delta H_{N+L} = \frac{\mathcal{E} \cdot \theta}{T_{c_2} - T_{c_1}} \left\{ \frac{\left(\frac{dT_c}{dt}\right)_1 + \left(\frac{dT_c}{dt}\right)_2}{2} - \frac{\Delta T_w \left[\left(\frac{dT_c}{dt}\right)_1 - \left(\frac{dT_c}{dt}\right)_2\right]}{\left(T_{j_1} - T_{j_2}\right) + \left(T_{c_2} - T_{c_1}\right)} \right\}$$

$$\Delta T_{corr} = \left(T_{c_2} - T_{c_1}\right) + \frac{\Delta T_w \cdot \theta}{T_{c_2} - T_{c_1}} \left[\left(\frac{dT_c}{dt}\right)_1 + \left(\frac{dT_c}{dt}\right)_2 \right]$$

$$C_p = \frac{\sum + \Delta H_{N+L}}{\Delta T_{corr}} = \frac{\mathcal{E}_{corr}}{\Delta T_{corr}}$$

where ΔH_{N+L} is the corrected heat transfer by Newton's Law and by heat leaking along the wires and supports; T_j is the temperature of the jacket; T_c is the temperature of the calorimeter; T_w is the difference between the surface temperature and the

assumed instantaneous temperature. The other symbols are denoted in Fig. 4. The details of the calculation are well described in Hawkins' thesis.[26]

C. Preparation of Alloys

(1) $In_{0.5}Pb_{0.5}$

510.039 grams of In and 921.959 gram of Pb were melted to give the equiatomic composition of the alloy. Indium of 99.999+% purity and lead of 99.999+% purity, both from the American Smelting and Refining Company, South Plainfield, New Jersey, were used. For both metals all impurities were reported to be below the 1 ppm level except for 3 ppm Cd and 2 ppm Pb in the indium.

The mixture of the two components was melted in an induction furnace at about 600°K under a helium atmosphere, then was poured into a chilled copper mold to form an ingot 1 inch in diameter and 12 inches long. The ingot was cold worked to increase the diffusion rate. Then the alloy was sealed in an evacuated glass tube with a reduced helium atmosphere and homogenized at 450°K for 7 days. Filings from both ends of the homogenized ingot were taken and strain annealed in boiling water for fifteen minutes then used for x-ray diffraction. The pattern from the diffractometer agrees well with the literature value.[16]

Back reflection lines show shapr peaks of the Cu-K_α doublets indicating good homogeneity. The ingot was cut into rods of 1/4 inch square and 5 inches long to fit into the calorimeter.

(2) $Au_{0.5}Cd_{0.5}$

99.999+% gold from Cominco American Inc., and 99.999+% cadmium from American Smelting and Refining Company were used. For both metals the spectrographic analysis showed that all impurities were below the 1 ppm level. Equiatomic amounts of the two components were weighed and sealed in a quartz tube under a reduced pressure (1/8 atm) of helium. The alloy was melted in several 200 gram batches. This mixture in the quartz tube was heated to 953°K (the melting point of the alloy is 900°K) in a vertical resistance furnace and was vigorously shaken after melting. After thorough mixing of the constituents, the quartz tube was quenched into an ice-water bath. The weight loss during melting ranged from 0.1% to 0.3%. The alloys then were homogenized in sealed silica tubes at 300°C, 450°C, and 550°C for one week at each temperature. Filings from samples of every batch were strain annealed and studied by x-ray diffraction. Sharp peaks at back reflection were obtained, showing good homogeneity. The line positions agreed well with literature values except for a few indefinite lines which might be

caused by a small amount of martensitic transformation into the tetragonal or orthorhombic structure near room temperature. A high temperature x-ray pattern at 350°C was taken. The lines were found to fit a CsCl structure with a = 3.333Å compare to 3.312Å of literature value[16] (also at 350°C). Metallographic study after the homogenization showed a single phase with large grains.

(3) Mg_3Sb_2

The alloys were made from 99.999+% sublimed Mg ingot obtained from Research Organic-Inorganic Chemical Company and 99.999+% antimony from the American Smelting and Refining Company which reported 3 ppm of bismuth in the antimony.

The alloy was difficult to make because the melting point of the alloy is very high, the alloy has a very high exothermic heat of formation, and Mg has a high vapor pressure. In the first two batches 50 grams of the mixture were melted. After confirming that the technique was successful in producing homogeneous alloys, 100-150 grams of the mixture were melted in each bath. A cylindrical graphite tube of 1 and 1/2 inches diameter was set inside an alumina tube placed in a vertical globar resistance furnace. Mg granules (about 5-10 mm) were first introduced into the graphite crucible and then crushed Sb

powder (about the same size as the Mg) was placed over the magnesium. The top of the alumina crucible was covered with a copper cap and vacuum sealed with an O-ring. The cap was cooled with running water. A stopper was placed at the bottom of the tube which is about 10 inches from the hot zone of the furnace. A copper tubing in the rubber stopper allowed the introduction of argon gas during the reactions. The furnace was slowly heated to 640°C (913°K), which is above the melting point of Sb (904°K) and below the melting point of Mg (922°K). Antimony first melted into the interstices of the Mg granules. The heat of the reaction melted the Mg, which further reacted with the antimony. The product became solid and was held at 640°C for 12 hours. After this the temperature was raised above the melting point of the alloy (about 1300°C). At this high temperature the melt was stirred about 50 times with a graphite rod by moving it up and down. The stirring rod was enlarged at the bottom to produce effective stirring. Finally, the melt was held at 1300°C for one hour. The furnace was then cooled to 870°C, which is 50° below the transformation temperature, and was held there for another 24 hours. The alloy was sealed into a quartz tube and annealed at 520°C for 7 days. There was about 0.5% weight loss during the melting.

The Nuclear Chemistry Department of the Lawrence Berkeley Laboratory analyzed the sample. From the analysis it was calculated that 0.6 weight percent of Mg and 0.2 weight percent of Sb were lost during the melting process. The precision of the analysis was ±0.1-0.3%. The analyzed alloy contained 0.4011 atomic fraction of antimony, practically the stoichiometric composition. The x-ray pattern agreed well with the literature values. The metallographic structure showed a very small amount of unreacted material which was found to be antimony by electron microprobe analysis. The alloy was pounded in a diamond mortar to a small size (about 0.5 cm in diameter, -100 mesh was removed) so the sample could be packed tighter to increase the heat conductivity.

III. EXPERIMENTAL RESULTS

A. InPb

About 100 measurements were made on 508.709 grams (3.1615 g-atom) of the InPb alloy. The experimental values are presented in Table 1. The smoothed values with the deviation, ΔC_p, from Kopp's law are presented in Table 2. Figure 5 shows the experimental values, the Kopp's law line (dotted line), and the smoothed curve of the heat capacity of the alloy (solid line). The change of ΔC_p with T is shown in Fig. 6. At low temperatures, around 30°K, ΔC_p shows a maximum value (0.32 cal/g-atom degree); it becomes negative above 130°K. Above 240°K was found an anomalous peak in C_p which reaches a maximum near 273°K and ends about 298°K. It is quite small; ΔH = 14 cal/g-atom degree, ΔS = 0.03 eu. The cause of the anomaly was not found. It is sluggish and depends on time and thermal history of the sample. The heat of the anomaly was obtained by heating the sample from 240°K to 300°K.

Three series of runs covering the anomaly region (240° to 300°K) were made, yielding different C_p values each time. The first series of the runs were made continuously from the liquid nitrogen temperature with little time interval between the measurements. The second series was made in the same way

TABLE I. Experimental Values for InPb

T, °K	Cp(cal/g-atom-deg)	T, °K	Cp(cal/g-atom-deg)
22.357	2.768	244.15	6.130
24.36	3.086	250.46	6.345
25.69	3.305	256.20	6.532
27.22	3.495	262.53	6.899
28.93	3.712	267.86	6.964
31.06	3.865	2nd Series	
33.92	4.074	234.30	6.227
37.99	4.283	244.34	6.336
47.61	4.775	254.12	6.437
59.12	5.182	260.26	6.581
65.73	5.381	266.15	6.543
70.27	5.487	271.99	6.508
76.46	5.589	276.47	6.426
80.33	5.617	280.05	6.420
83.79	5.636	285.90	6.400
88.05	5.676	291.80	6.394
94.10	5.743	3rd Series	
100.16	5.774	232.43	6.104
106.87	5.812	236.05	6.176
112.18	5.841	240.24	6.192
120.73	5.843	247.04	6.306
126.94	5.904	250.21	6.320
135.56	6.020	253.22	6.372
142.38	6.006	256.21	6.454
150.37	6.039	259.07	6.582
157.82	6.044	262.13	6.686
164.27	6.016	265.13	6.716
170.38	6.018	268.14	6.919
176.46	6.015	270.24	6.852
185.25	6.016	272.26	6.826
193.24	6.047	274.18	6.813
198.51	6.042	277.02	6.733
202.04	6.053	280.02	6.655
206.50	6.092	285.07	6.571
210.03	6.125	290.36	6.441
214.48	6.104	295.30	6.392
220.47	6.167	300.05	6.282
227.88	6.196		
232.88	6.196		
238.49	6.220		

TABLE II. Smoothed Values for InPb

T, °K	C_p (cal/g-atom-deg)	ΔC_p (cal/g-atom-deg)	T, °K	C_p (cal/g-atom-deg)	ΔC_p (cal/g-atom-deg)
20	2.406	0.236	140	5.952	-0.018
25	3.185	0.300	150	5.978	-0.036
30	3.788	0.328	160	6.003	-0.052
35	4.205	0.280	170	6.015	-0.070
40	4.505	0.220	180	6.031	-0.084
45	4.749	0.184	190	6.049	-0.096
50	4.944	0.164	200	6.069	-0.106
55	5.103	0.148	210	6.088	-0.112
60	5.231	0.136	220	6.104	-0.116
65	5.341	0.126	230	6.128	-0.117
70	5.436	0.116	240	6.153	-0.117
75	5.511	0.106	250	6.335	0.050
80	5.576	0.096	260	6.620	0.320
85	5.636	0.086	270	6.890	0.570
90	5.686	0.076	280	6.660	0.320
95	5.726	0.066	290	6.475	0.120
100	5.767	0.057	298.15	6.380	0.000
110	5.824	0.039	300	6.375	0.000
120	5.880	0.020			
130	5.915	0.000			

$S_{st}-S_0 = 15.179$ eu $\quad \Delta S_{st}-\Delta S_0 = 0.494$ eu

$H_{st}-H_0 = 1626$ cal/g-atom $\quad \Delta H_{st}-\Delta H_0 = 13$ cal/g-atom

Of these the anomaly accounts for

$\Delta S = \sim 0.030$ eu

$\Delta H = \sim 14$ cal/g-atom

Note: subscript st means standard temperature, 298.15°K

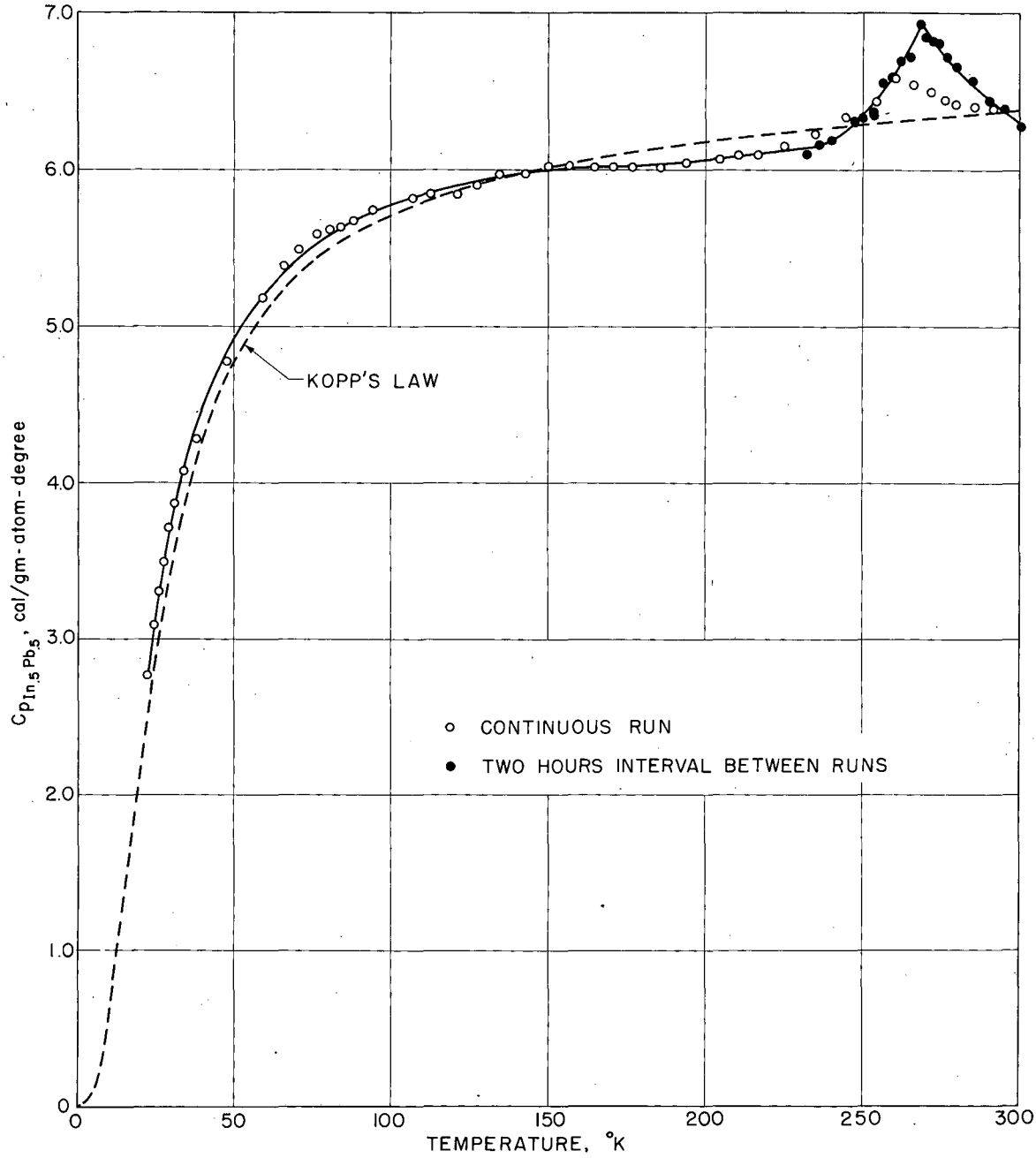

FIG. 5 HEAT CAPACITY OF InPb

XBL716-6901

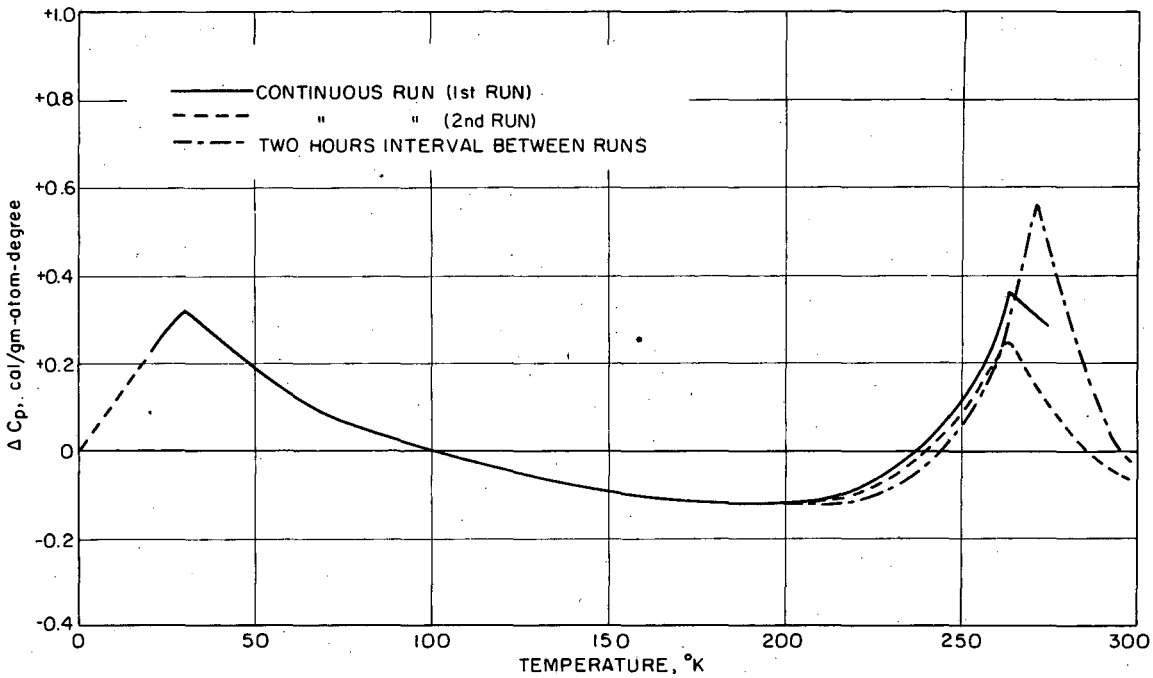

FIG. 6 DEVIATION FROM KOPP'S LAW FOR InPb

XBL716-6902

as the first series yielding a somewhat different anomaly. The third series was made with two hour intervals between the measurements to give enough time to reach equilibrium; the anomaly was still higher. The series with different time intervals between measurements are shown in Fig. 7. To obtain the value at the peak, 275°K, the samples were held at ice temperature for one day, three days, and one week, respectively, without changing the measured value of C_p at the ice point, showing one day was long enough to reach equilibrium. The sample was held at room temperature for one week. The C_p value at room temperature agrees well with the smoothed value which is extrapolated to this temperature from below the anomaly, showing that the anomaly is completed at room temperature. The classic λ-shape of the anomaly was not found, possibly due to difficulties of reaching equilibrium.

The x-ray pattern at liquid nitrogen temperature is nearly identical with that at room temperature except for a small shift of the lines due to thermal contraction of the crystal. Thus the anomaly does not come from a structure change, not even from a change of the c/a ratio. Similar unexplained anomalies have been found in hexahydrates of magnesium chloride ($MgCl_2 \cdot 6H_2O$) and γ-maganese.[28] The results of integration by Simpson's rule are given in Table 2.

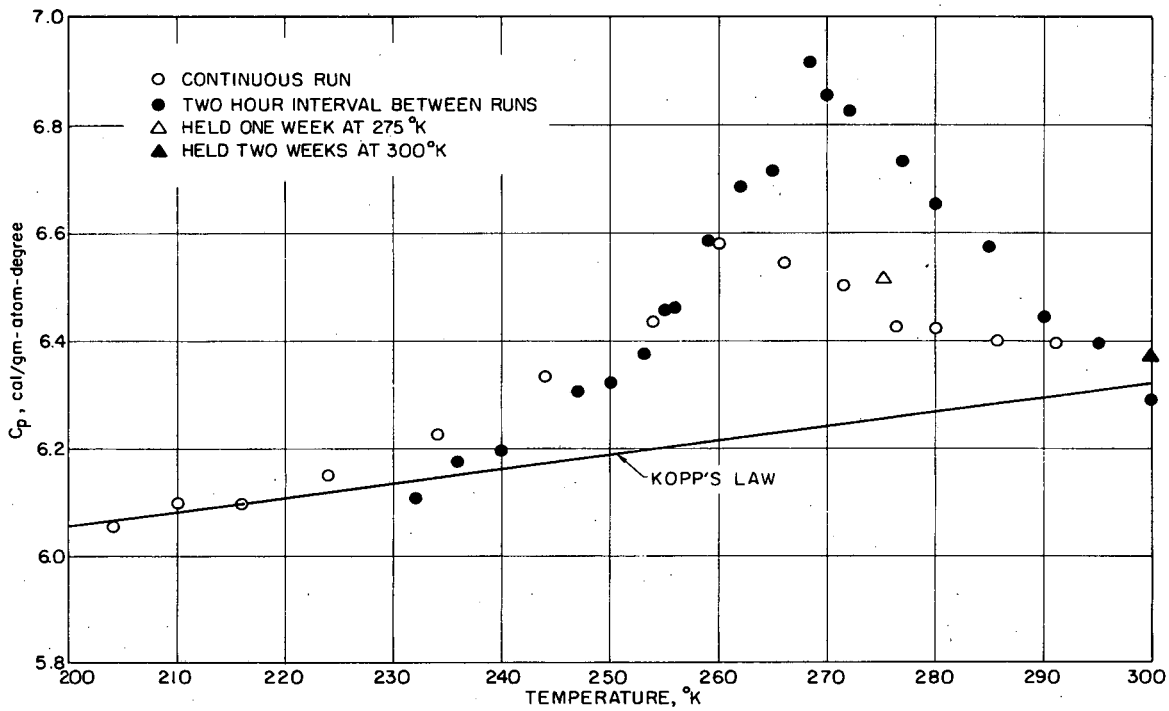

FIG. 7 ANOMALY PORTION OF THE HEAT CAPACITY OF InPb

XBL716-6903

TABLE III. Equilibrium Measurements

Holding Period	T,°K	Cp(cal/g-atom-deg)
one day	277.12	6.415
three days	274.84	6.491
one week	275.42	6.511
two weeks	300.80	6.384

B. AuCd

Fifty-two measurements were made on a 696.319 g (4.5026 g-atom) sample of AuCd. The experimental data are presented in Table 4. The smoothed values and ΔC_p are presented in Table 5. Figure 8 shows the experimental points, the smoothed values and the Kopp's law values for the alloy. The smoothed values were obtained by drawing a smoothed curve on the ΔC_p plot, extrapolating this smooth curve from 20°K to 0°K, and adding these smoothed ΔC_p values to the Kopp's law values. The ΔC_p curve is shown in Fig. 9. ΔC_p is zero at 20°K and decreases to -0.08 cal/g-atom-deg near 60°K. Above 200°K the deviation becomes positive up to room temperature. The maximum positive deviation is about 0.1 cal/g-atom-deg. near room temperature. The integration of the smoothed values are given in Table 5. Kubaschewski measured $H_T - H_{st}$ for the congruent melting composition of the β-phase between 608°-1034°K. From this measurement he obtained a negative ΔC_p, which is not consistent with this study.

B. Mg_3Sb_2

Forty-eight measurements were made on 226.631 g (3.5805 g-atom) of Mg_3Sb_2. The experimental values are presented

TABLE IV. Experimental Values for AuCd

T,°K	Cp(cal/g-atom-deg)	T,°K	Cp(cal/g-atom-deg)
23.75	1.381	143.77	5.633
25.47	1.628	151.81	5.661
27.18	1.817	157.85	5.680
28.69	1.886	163.91	5.738
30.67	2.190	171.00	5.749
36.91	2.625	176.15	5.733
40.14	2.858	183.68	5.752
44.87	3.170	192.03	5.837
49.85	3.538	198.19	5.864
54.91	3.829	201.69	5.917
60.26	4.124	205.59	5.934
66.24	4.379	211.79	5.974
72.68	4.590	218.22	5.947
76.11	4.687	223.68	6.002
79.26	4.717	229.79	6.002
83.76	4.849	237.79	6.028
88.17	4.967	244.20	6.056
92.23	5.045	250.60	6.085
99.04	5.151	256.26	6.083
103.88	5.215	256.40	6.094
111.12	5.305	261.84	6.153
114.73	5.339	267.81	6.117
119.32	5.383	273.93	6.189
125.51	5.456	279.91	6.210
131.67	5.543	285.98	6.232
137.81	5.640	291.91	6.232

TABLE V. Smoothed Values for AuCd

T, °K	Cp (cal/g-atom-deg)	ΔCp	T, °K	Cp (cal/g-atom-deg)	ΔCp
20	1.035	0.036	130	5.502	-0.055
25	1.546	0.036	140	5.584	-0.048
30	2.052	0.024	150	5.658	-0.042
35	2.493	-0.014	160	5.718	-0.032
40	2.893	-0.052	170	5.768	-0.024
45	3.267	-0.065	180	5.879	-0.014
50	3.588	-0.074	190	5.863	-0.002
55	3.857	-0.078	200	5.908	0.008
60	4.080	-0.080	210	5.943	0.018
65	4.282	-0.080	220	5.979	0.029
70	4.453	-0.082	230	6.011	0.039
75	4.605	-0.082	240	6.049	0.049
80	4.747	-0.080	250	6.084	0.059
85	4.865	-0.078	260	6.115	0.068
90	4.970	-0.077	270	6.148	0.078
95	5.064	-0.074	280	6.175	0.085
100	5.152	-0.072	290	6.207	0.092
110	5.296	-0.064	298.15	6.221	0.096
120	5.405	-0.062	300	6.225	0.098

$S_{st} - S_0 = 11.837$ eu

$\Delta S_{st} - \Delta S_0 = -0.028$ eu

$H_{st} - H_0 = 1463$ cal/g-atom

$\Delta H_{st} - \Delta H_0 = -14$ cal/g-atom

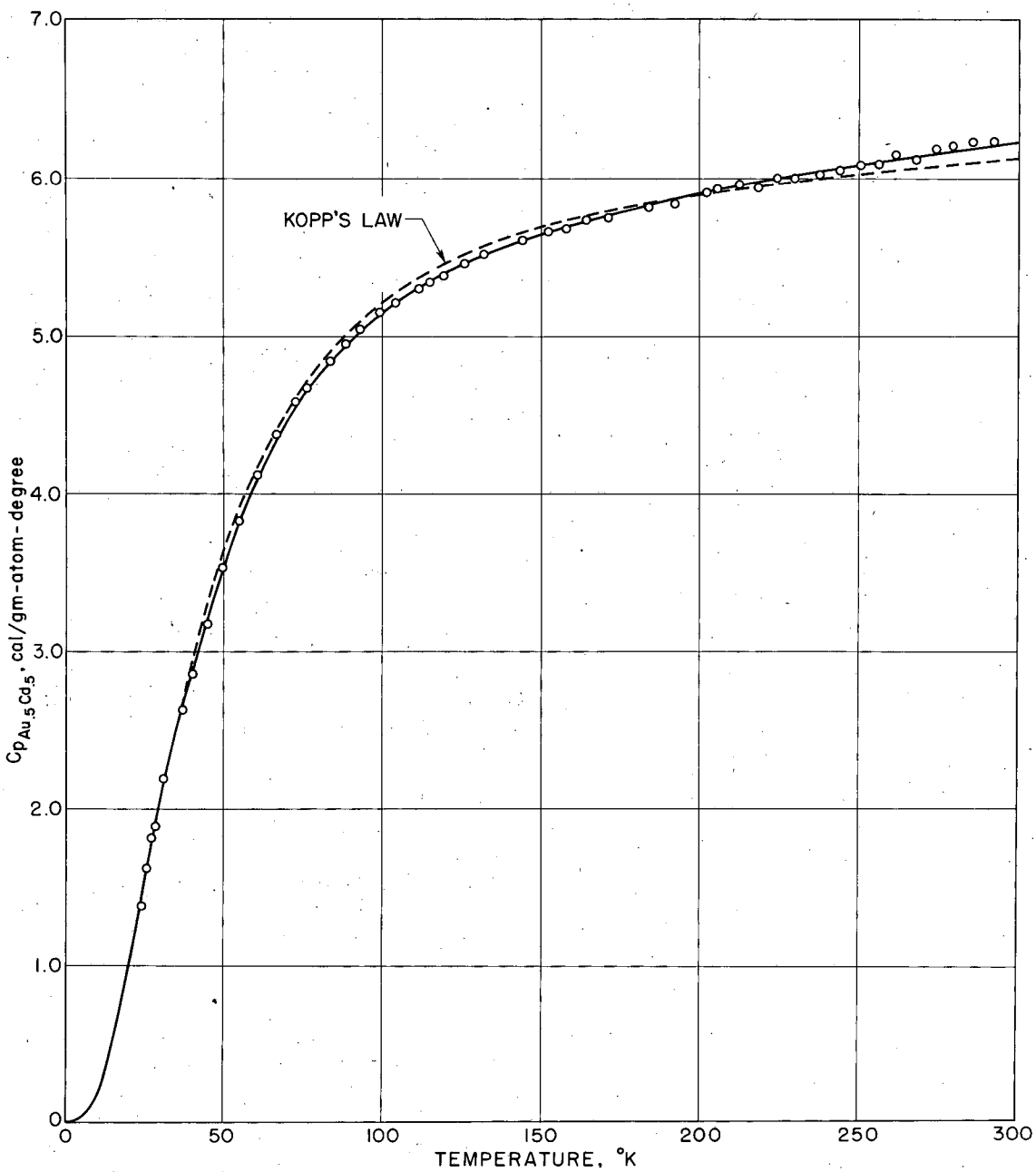

FIG. 8 HEAT CAPACITY OF Au Cd

XBL716-6904

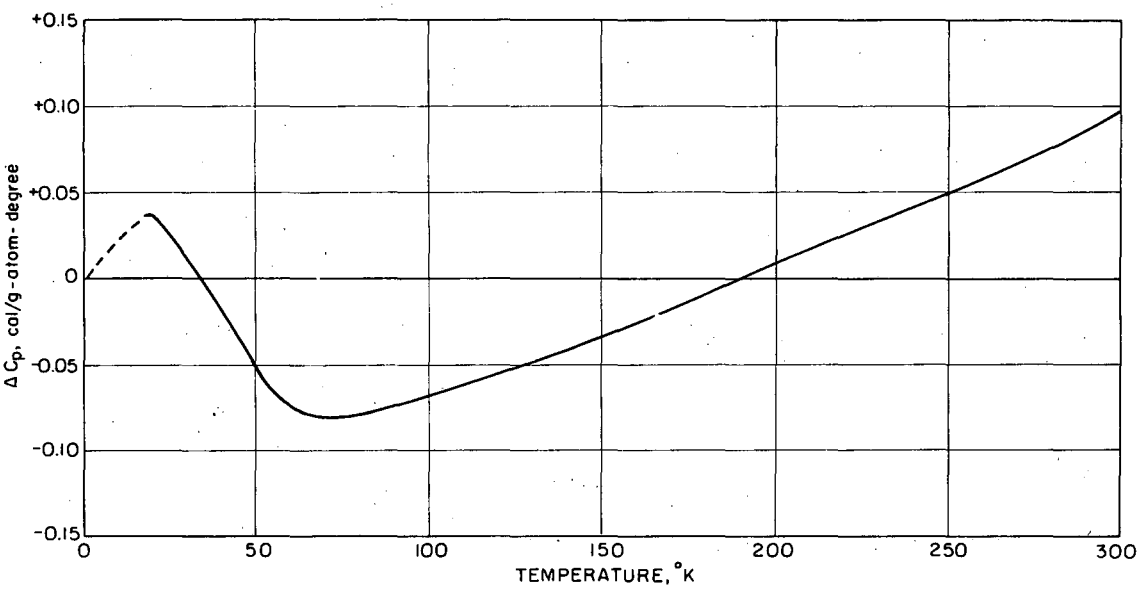

FIG. 9 DEVIATION FROM KOPP'S LAW FOR AuCd

XBL 716-6912

in Table 6 and the smoothed values along with ΔC_p are presented in Table 7. Figure 10 shows the experimental values, the Kopp's law line and the smoothed values of the C_p curve of the alloy. The smoothed curve was taken the same way as was that for the AuCd alloy. Figure 11 shows a large negative deviation of ΔC_p at room temperature (-0.292 cal/g-atom-deg) and a maximum positive deviation near 30°K. The curve crosses the Kopp's law line at 70°K.

Integration of this smoothed curve are given in Table 7. The expression of Born and Von Karman[29] on heat capacity had been used to fit the heat capacity curve of the alloy. With some modification, assuming isotropicity of the alloy and neglecting the dialtion term,[30] the following expression was found to fit the curve:

$$C_{p\,Mg_3Sb_2} = D(108/T) + 2E(156/T) + 2E(338/T)$$

where $D(\theta_D/T)$ and $E(\theta_E/T)$ represent, respectively, Debye and Einstein heat capacity functions.

TABLE VI. Experimental Values for Mg_3Sb_2

T, °K	Cp(cal/g-atom-deg)	T, °K	Cp(cal/g-atom-deg)
24.81	0.695	142.05	4.853
26.97	0.850	156.58	4.964
28.65	0.972	162.12	5.078
30.25	1.073	169.18	5.158
32.02	1.170	181.85	5.218
35.88	1.383	188.04	5.250
39.94	1.586	193.85	5.285
44.90	1.819	198.96	5.316
55.35	2.418	202.72	5.377
60.42	2.678	206.73	5.375
66.73	2.971	210.61	5.397
72.36	3.168	214.41	5.392
77.32	3.380	220.60	5.453
82.50	3.563	226.56	5.484
86.31	3.673	236.13	5.494
89.75	3.778	242.67	5.506
94.05	3.864	246.95	5.532
99.79	4.046	258.51	5.586
105.87	4.186	270.67	5.576
111.94	4.324	277.91	5.593
117.89	4.436	283.98	5.628
123.91	4.542	289.86	5.671
130.17	4.672	295.97	5.673
136.14	4.756		

TABLE VII. Smoothed Values for Mg_3Sb_2

T, °K	Cp (cal/g-atom-deg)	ΔCp	T, °K	Cp (cal/g-atom-deg)	ΔCp
20	0.466	0.114	130	4.662	-0.204
25	0.735	0.155	140	4.807	-0.217
30	1.020	0.176	150	4.925	-0.227
35	1.300	0.165	160	5.031	-0.237
40	1.580	0.139	170	5.119	-0.245
45	1.865	0.111	180	5.198	-0.252
50	2.148	0.080	190	5.265	-0.257
55	2.410	0.050	200	5.324	-0.262
60	2.654	0.020	210	5.376	-0.267
65	2.880	-0.010	220	5.421	-0.273
70	3.099	-0.038	230	5.461	-0.277
75	3.297	-0.062	240	5.498	-0.281
80	3.474	-0.088	250	5.536	-0.284
85	3.638	-0.110	260	5.570	-0.285
90	3.796	-0.126	270	5.605	-0.286
95	3.954	-0.138	280	5.635	-0.288
100	4.080	-0.150	290	5.663	-0.290
110	4.297	-0.171	298.15	5.685	-0.291
120	4.495	-0.188	300	5.690	-0.292

$S_{st} - S_0 = 8.753$ eu

$\Delta S_{st} - \Delta S_0 = -0.072$ eu

$H_{st} - H_0 = 1228$ cal/g-atom

$\Delta H_{st} - \Delta H_0 = -50$ cal/g-atom

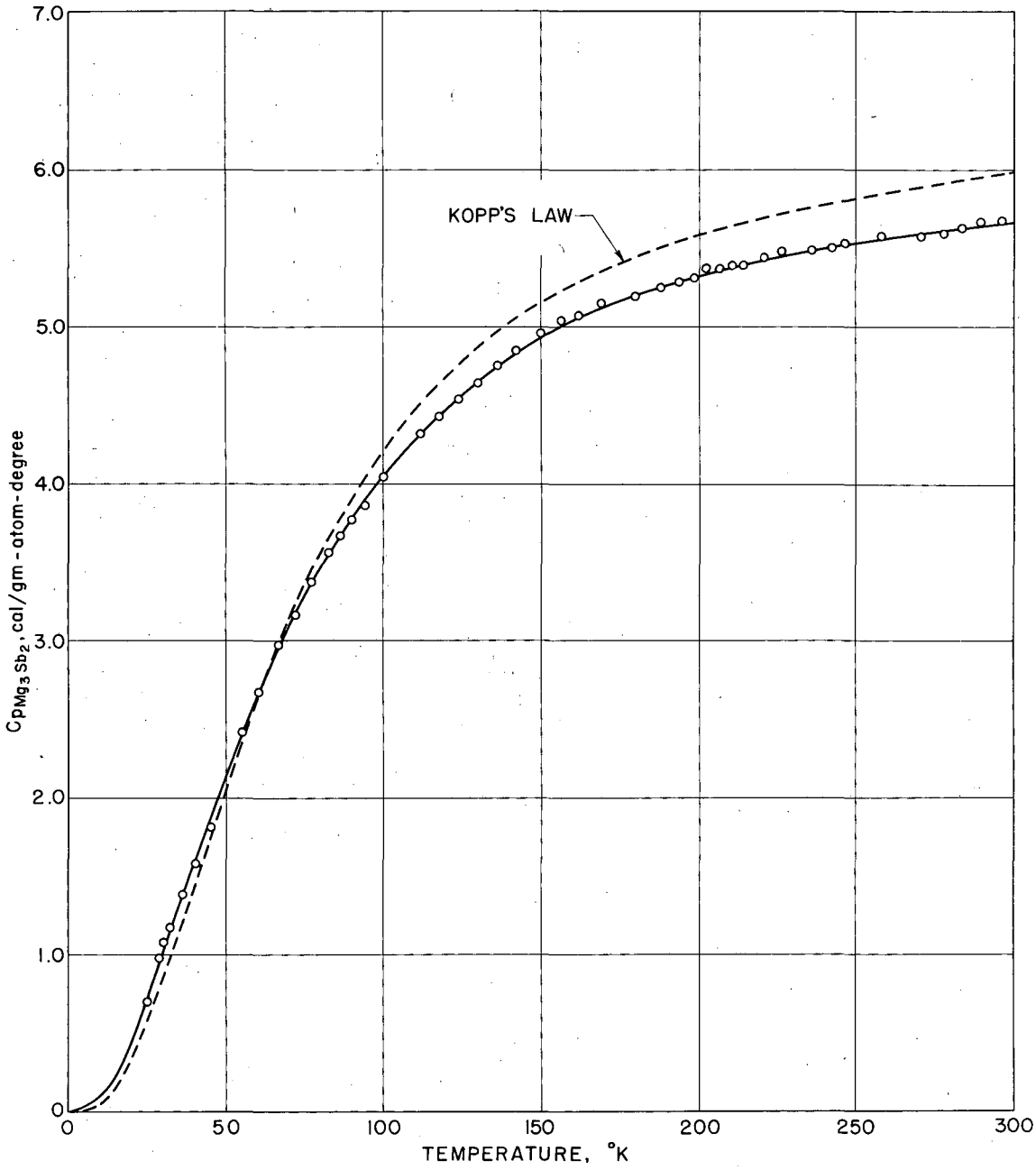

FIG. 10 HEAT CAPACITY OF Mg_3Sb_2

XBL716-6905

IV. DISCUSSION

It would be expected that when dissimilar atoms attract each other (larger bonding energy than the average of pure components), the system becomes exothermic and when dissimilar atoms have a lower bonding energy than average, the system would become endothermic if other factors do not interfere. Therefore, one would expect a higher vibrational frequency than the average of the pure components in exothermic systems and a lower vibrational frequency in endothermic systems.

The bonding energy could be generally referred to the size and sign of the heat of formation. The higher vibrational frequency relates to a higher Debye temperature and thus to a lower heat capacity. The size and sign of the deviation of heat capacity from the Kopp's law value determine the thermal entropy. The effects found here were rather small. A positive vibrational entropy of formation was obtained in the endothermic InPb alloy, a very small negative value in the moderately exothermic AuCd, and a small but definite negative value for the highly exothermic Mg_3Sb_2 alloy. The small negative vibrational entropy of formation in the Mg_3Sb_2 alloy (Table 7) consisted of a large positive deviation at low temperatures cancelling most of the negative contribution to the

vibrational entropy at higher temperatures. Consequently $(\Delta H_{st}-\Delta H_0)$ show the negative values of ΔC_p more clearly than does the entropy. The AuCd alloy shows small negative deviation at low temperatures and small positive deviations above 200°K. It is noteworthy that ΔC_p was positive at low temperatures for Mg_3Sb_2 even though it is highly exothermic system. The Mg_3Sb_2 alloy showed a relatively large negative $(\Delta H_{st}-\Delta H_0)$ value (-50 cal/g-atom) compared with AuCd (-14 cal/g-atom) and InPb (-1 cal/g-atom).

In general, highly exothermic substitutional alloys have a negative $(\Delta H_{st}-\Delta H_0)$, but much more work is needed for endothermic systems for further confirmation. Alloys containing transition metals would possibly show deviation from this general trend because of the possible secondary effects due to electronic and magnetic transitions. Some more work on different systems with a medium range of exothermic heats of formation would confirm and extend the present results. To make sure of the nature of the anomaly in the InPb alloy, other measurements of different compositions of the phase are needed.

Part 2. EFFECT OF ORDERING ON LATTICE HEAT CAPACITY: $AuCu_3$

I. INTRODUCTION

The effect of the order-disorder transformation on lattice vibrational heat capacities has not been much studied. Hawkins and Hultgren[12] found for AuCu that the differences in low temperature C_p between the ordered and disordered state were not great. They found slightly higher C_p in the disordered state at low temperatures while at high temperatures the C_p of the ordered state was a little higher. The cross over came at around 100°K. The effect of ordering on the electronic heat capacity was studied by Rayne[31] and Martin[32] (below 4.2°K) on the $AuCu_3$ alloy. They found substantially no change, suggesting little change in the density of states of the Fermi electron gas on ordering. However, they did find a small increase of the Debye characteristic temperature of the lattice on ordering. Their Debye temperatures along with Flinn's calculation[33] from elastic constant measurements for both ordered and disordered states of the $AuCu_3$ alloy are as follows:

	Quenched	Ordered
Rayne	278 ± 2°K	285 ± 2°K
Martin	269 ± 0.5°K	285 ± 0.8°K
Flinn	281 ± 35°K	283 ± 3.5°K

Remarkable agreement in heat capacity from direct measurements and from elastic constant measurements was found in the ordered state; less good agreement was found in the disordered state. This result is not surprising considering the fact that the atom arrangements in ordered state are better defined permitting better calculation. Moreover, in the disordered state, extra vibrations of low frequencies are expected. According to Rosenstock[34] these lower than average frequencies in the disordered state come from the loosely bound atoms. For the case of quartz[35] and vitreous silica (which has the same chemical composition but is disordered), this evidence of extra heat capacity in the disordered state has been found. Also vitreous selenium[36] has extra heat capacity above crystalline selenium.

Lattice heat capacities are of great interest because the bond strength between the atoms can be qualitatively inferred. They are also of interest to obtain absolute entropies and the zero point entropy with the aid of high temperature data.

Sattherthwaite, Craig, and Wallace[10] and Coffer, Craig, Krier, and Wallace[11] measured the heat capacity of ordered Cd-Mg alloys but made no measurements on disordered samples. At temperatures near the order-disorder critical point, one

would expect the C_p of the ordered state to be higher than that of the disordered state due to the onset of disordering. However, this is hardly a cause of the increased heat capacity of the ordered state at the low temperatures measured by Hawkins and Hultgren[12] because disordering does not start below about 500°K.

The purpose of this study is to investigate further the effect of ordering on lattice heat capacity and to verify the result found for the AuCu alloy.

$AuCu_3$ was chosen because it is very similar to AuCu and much is known of its high-temperature properties. Furthermore the lattice structure remains cubic on ordering; gold and copper are in the same column of the periodic table, and form continuous solid solutions. High temperature heat and entropy of formation measurements at 800°K are available as well as measurements of heat of formation as a function of temperature from 298.15° to 800°K. According to Hansen,[17] Au and Cu form a completely miscible series of disordered solutions with a face centered cubic (A1) structure. The ordered structure of $AuCu_3$ is formed below 663°K and has a cubic ($L1_2$) prototype structure. Although the quenched alloy may appear from the x-ray pattern to be completely disordered, considerable short-range order could exist.

Heats of formation measurements by the liquid tin solution calorimeter provide the method of determining the degree of disorder of the sample. The low temperature isothermal calorimeter used in this study is the same as the one described in the first section of this thesis.

II. EXPERIMENTAL

The alloy was made from American Smelting and Refining Company 99.999% pure copper and Cominco American Inc. 99.999% pure gold. Spectrographic analysis showed all impurities were less than 1 ppm for both metals except that copper had 2 ppm tellurium impurity.

935.947 grams of copper and 967.145 grams of gold were melted together near 1200°C in a graphite crucible in an induction furnace under a reduced pressure of helium, then chill cast into a copper mold to form an ingot 1 inch in diameter and 6 inches long. The top of the ingot was cut off. Filings from both ends were mixed and given a short strain-anneal, then quenched. X-ray diffraction patterns showed sharp lines on back reflection, proving the sample was homogeneous. The ingot was sawed into rod shapes so that it could easily be put into the calorimeter.

To make the ordered sample, rods of the alloy were sealed into a quartz tube under a reduced helium atmosphere, held at 620°K for 4 days, slowly cooled to 400°K over a period of 4 days by reducing the furnace temperature about 25°C every 12 hours, then furnace cooled. The rods were x-rayed. The x-ray pattern showed sharp superlattice lines of the cubic structure, indicating

that the sample was well ordered. After the measurements of C_p of the ordered $AuCu_3$ alloy, it was heat treated to give a disordered state. Each rod was sealed in a small quartz tube to give faster contact with the ice-water bath when quenching, and held at 750°K for 10 days. Each rod sample was then quenched into an ice-water bath. The x-ray pattern of the rods showed no superlattice lines, indicating the absence of long-range order. At the same time pellets were prepared by the same heat treatments. Heats of formation of the pellets were determined in order to estimate the degree of disorder of the sample.

III. EXPERIMENTAL RESULTS

Sixty-five measurements of C_p were made on 722.666 grams (7.4581 g-atom) of ordered $AuCu_3$ alloy. The experimental values are given in Table 8 and the smoothed values together with deviations from Kopp's law (ΔC_p) are presented in Table 9. These smoothed values and the Kopp's law line (dotted line) together with experimental values are shown in Fig. 12. ΔC_p values were smoothed and this smoothed line was extrapolated from 20°K to 0°K. The smoothed ΔC_p values were added to the Kopp's law values to give smoothed C_p values to 0°K. The values of $S_{st}-S_0$ and $H_{st}-H_0$ were obtained by integration of the smoothed curve using Simpson's rule. The smoothed ΔC_p curve is shown in Fig. 13. This curve has a maximum positive value at 75°K (0.1 cal/g-atom-degree), crosses over the Kopp's law line at 150°K to reach negative values at room temperature of the order of 0.08 cal/g-atom-degree.

Another 65 determinations were made on 672.430 grams (6.9396 g-atom) of the quenched (disordered) alloy. Experimental data are given in Table 10, smoothed values in Table 9 together with deviations from Kopp's law values. The experimental points, the smoothed curve (solid line), and the Kopp's law line (dotted line) are shown in Fig. 14. Figure 15 shows the ΔC_p curve, versus temperature.

TABLE VIII. Experimental Results for Ordered $AuCu_3$

T, °K	Cp(cal/g-atom-deg)	T, °K	Cp(cal/g-atom-deg)
25.54	0.508	154.03	5.187
27.06	0.597	160.02	5.205
28.30	0.668	166.09	5.259
29.54	0.753	171.85	5.325
31.06	0.805	177.85	5.363
33.37	0.982	183.86	5.372
36.62	1.166	189.80	5.419
39.97	1.397	197.42	5.432
44.68	1.649	202.26	5.489
49.75	1.992	206.12	5.492
55.07	2.336	209.58	5.505
61.22	2.689	213.74	5.520
67.04	3.003	217.92	5.538
73.07	3.323	222.05	5.558
78.95	3.546	226.61	5.547
84.08	3.723	231.10	5.622
87.41	3.858	235.32	5.628
91.43	3.991	240.26	5.653
95.99	4.119	250.05	5.682
101.60	4.284	258.74	5.736
107.74	4.404	262.04	5.725
113.82	4.505	266.76	5.760
119.83	4.649	271.62	5.772
126.08	4.780	277.54	5.800
132.14	4.847	283.97	5.805
136.41	4.972	289.64	5.804
142.11	5.027	295.65	5.832
148.01	5.087		

TABLE IX. Smoothed Values for $AuCu_3$

	ORDERED			DISORDERED	
T, °K	Cp (cal/g-atom-deg)	ΔCp	T, °K	Cp (cal/g-atom-deg)	ΔCp
20	0.284	0.019	20	0.302	0.038
25	0.509	0.024	25	0.533	0.048
30	0.771	0.030	30	0.801	0.060
35	1.073	0.037	35	1.107	0.070
40	1.398	0.047	40	1.434	0.082
45	1.731	0.065	45	1.762	0.096
50	2.044	0.085	50	2.069	0.110
55	2.354	0.097	55	2.382	0.125
60	2.634	0.104	60	2.671	0.141
65	2.902	0.108	65	2.949	0.155
70	3.142	0.107	70	3.200	0.165
75	3.349	0.105	75	3.409	0.165
80	3.583	0.102	80	3.636	0.155
85	3.759	0.096	85	3.805	0.142
90	3.930	0.090	90	3.969	0.129
95	4.090	0.083	95	4.123	0.116
100	4.234	0.077	100	4.261	0.104
110	4.471	0.064	110	4.488	0.081
120	4.669	0.052	120	4.677	0.060
130	4.835	0.039	130	4.836	0.040
140	4.978	0.027	140	4.972	0.021
150	5.101	0.014	150	5.092	0.005
160	5.194	0.002	160	5.182	-0.010
170	5.283	-0.011	170	5.271	-0.023
180	5.349	-0.024	180	5.340	-0.035
190	5.417	-0.037	190	5.409	-0.045
200	5.461	-0.049	200	5.455	-0.055
210	5.509	-0.060	210	5.506	-0.063
220	5.555	-0.067	220	5.552	-0.070
230	5.600	-0.070	230	5.594	-0.076
240	5.645	-0.067	240	5.630	-0.081
250	5.690	-0.063	250	5.670	-0.083
260	5.726	-0.059	260	5.703	-0.083
270	5.762	-0.054	270	5.736	-0.080
280	5.794	-0.049	280	5.770	-0.074
290	5.829	-0.043	290	5.806	-0.067
298.15	5.856	-0.039	298.15	5.835	-0.062
300	5.863	-0.038	300	5.842	-0.059

TABLE IX. (Continued)

ORDERED	DISORDERED
$S_{298.15} - S_0 = 8.880$ eu	$S_{298.15} - S_0 = 8.945$ eu
$H_{298.15} - H_0 = 1258$ cal/g-atom	$H_{298.15} - H_0 = 1259$ cal/g-atom
$\Delta S_{298.15} - \Delta S_0 = 0.100$	$\Delta S_{298.15} - \Delta S_0 = 0.165$

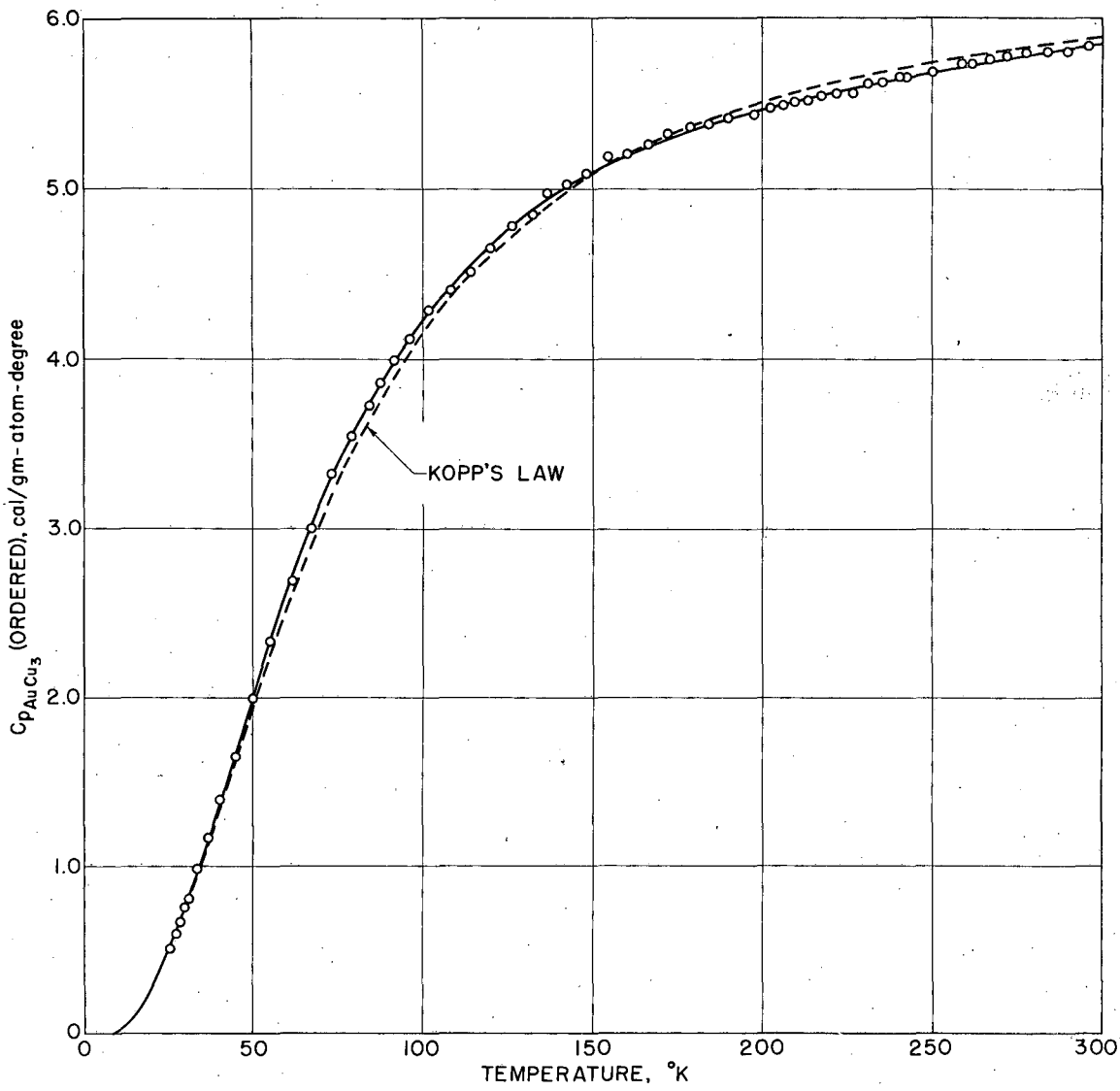

FIG. 12 HEAT CAPACITY OF ORDERED $AuCu_3$

XBL716-6907

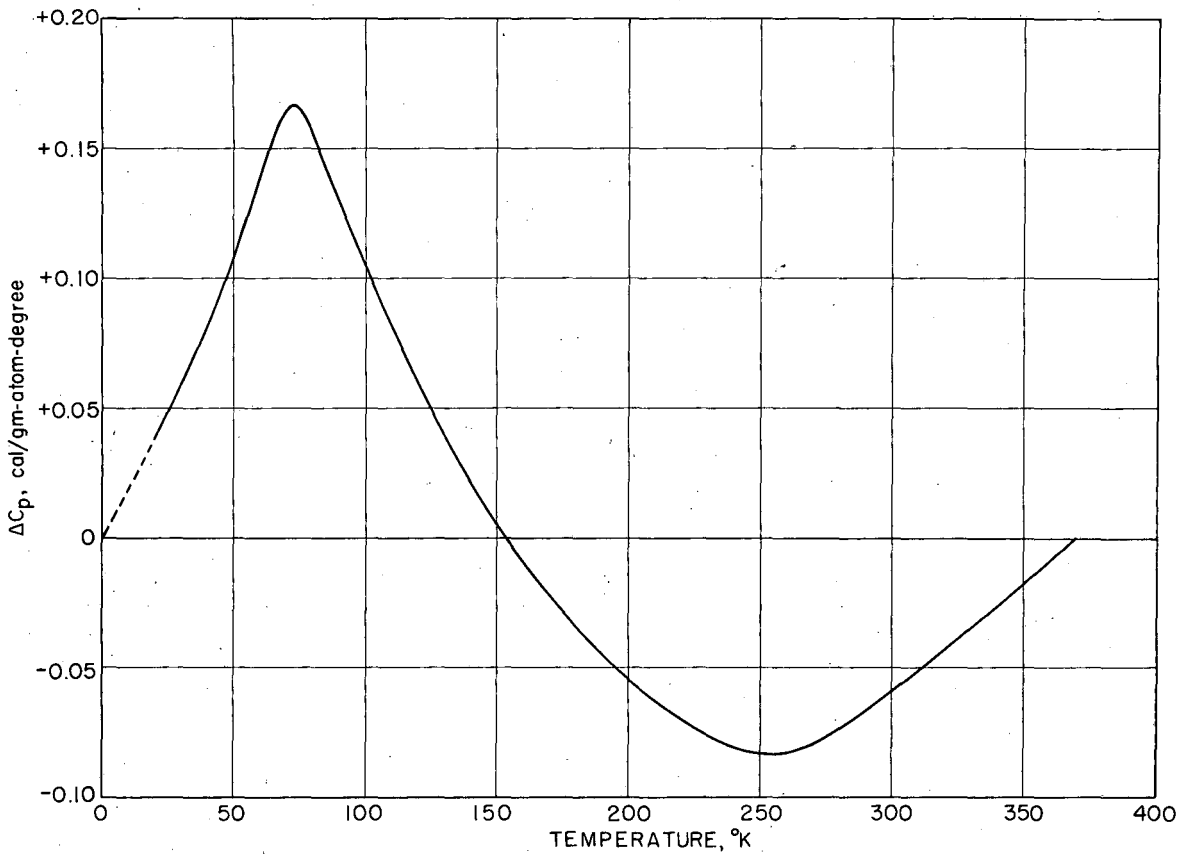

FIG. 13. DEVIATION FROM KOPP'S LAW FOR DISORDERED $AuCu_3$

XBL 716-6908

TABLE X. Experimental Results for Disordered $AuCu_3$

T, °K	Cp(cal/g-atom-deg)	T, °K	Cp(cal/g-atom-deg)
23.65	0.459	143.59	5.026
25.68	0.554	149.82	5.097
27.02	0.630	155.85	5.186
28.36	0.707	161.62	5.213
29.77	0.803	167.45	5.232
31.68	0.919	169.90	5.276
33.90	1.058	173.67	5.292
40.00	1.400	179.85	5.338
45.72	1.765	184.39	5.352
51.63	2.143	192.19	5.382
58.45	2.565	198.22	5.454
63.78	2.816	205.86	5.486
69.59	3.128	211.57	5.503
75.92	3.455	215.66	5.547
81.51	3.596	221.48	5.564
80.20	3.664	225.50	5.613
83.51	3.703	229.99	5.614
87.34	3.870	235.73	5.648
91.51	4.008	241.82	5.636
95.65	4.159	247.81	5.683
101.59	4.286	253.65	5.678
107.45	4.395	259.65	5.685
110.93	4.530	265.97	5.710
114.32	4.580	271.74	5.730
119.59	4.652	279.46	5.796
126.04	4.757	286.39	5.786
131.55	4.859	289.42	5.804
137.63	4.926	295.51	5.795

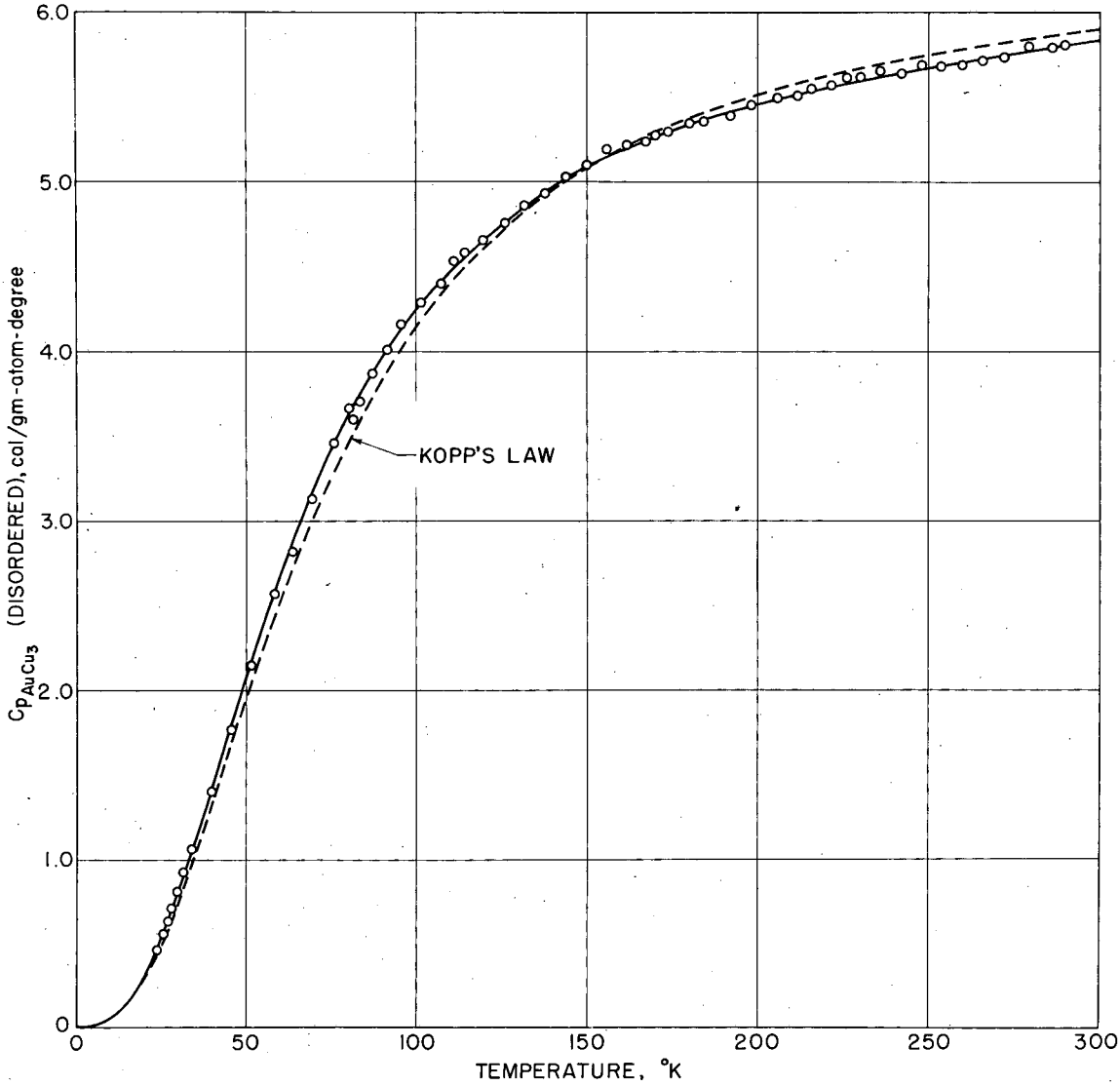

FIG. 14 HEAT CAPACITY OF DISORDERED $AuCu_3$

XBL716-6909

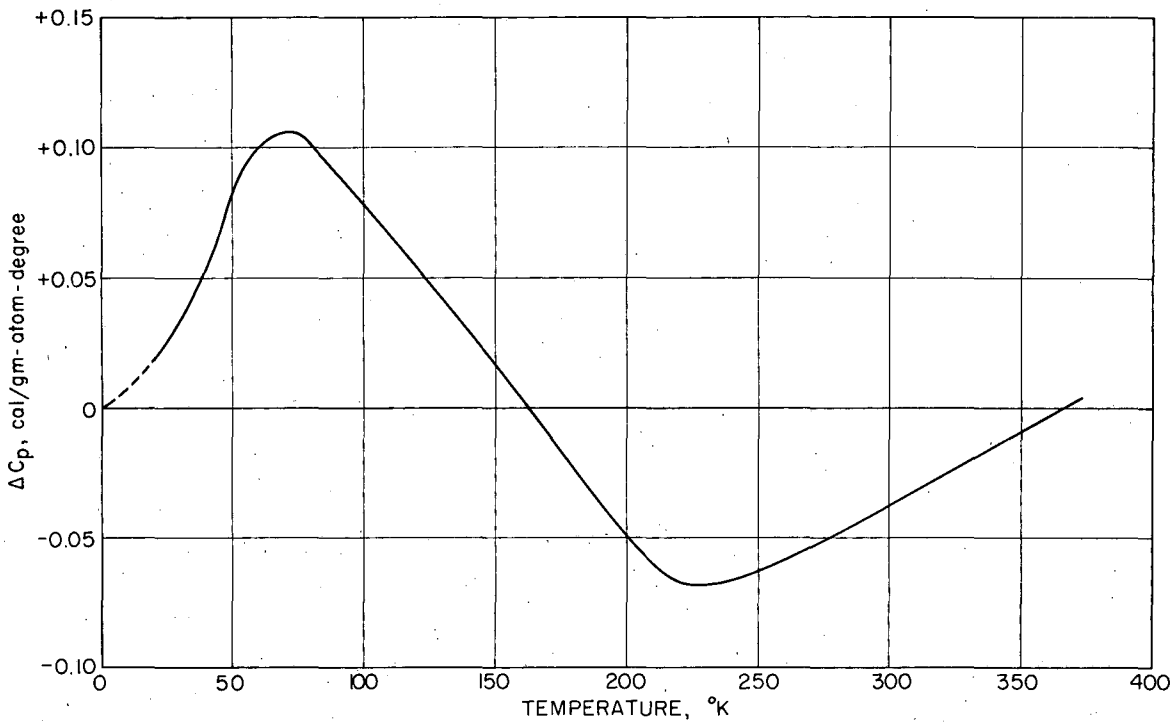

FIG. 15 DEVIATION FROM KOPP'S LAW FOR ORDERED $AuCu_3$

XBL 716-6910

$\Delta S_{st}-\Delta S_0$ and $\Delta H_{st}-\Delta H_0$ were calculated using the values for Au and Cu from Hultgren et al.[1] The C_p curve of the disordered state also shows a positive deviation at low temperatures (the maximum comes at 75°K) and a slightly negative deviation at high temperatures. Both smoothed curves of the ordered state and disordered state were plotted in Fig. 16 with the Kopp's law line.

The runs on pure gold by Hawkins were studied to see if there are any systematic errors. The agreement with the selected values was good but there was little systematic deviation at low temperatures. These deviations from selected values were positive with a maximum at 75°K, which is the same temperature where the maximum deivation from Kopp's law comes for the both ordered and disordered states. The magnitude of the maximum discrepancy from selected values on gold is near the maximum deviation from Kopp's law for the ordered state. This discrepancy could be a systematic error, which could result from a deviation of the temperature scale.

High-Temperature Data

The heats of formation of the quenched sample were measured in a liquid tin solution calorimeter at 315°K in the same way as done by Orr.[37] The measured value is ΔH_f = -1150 cal/g-atom. Orr

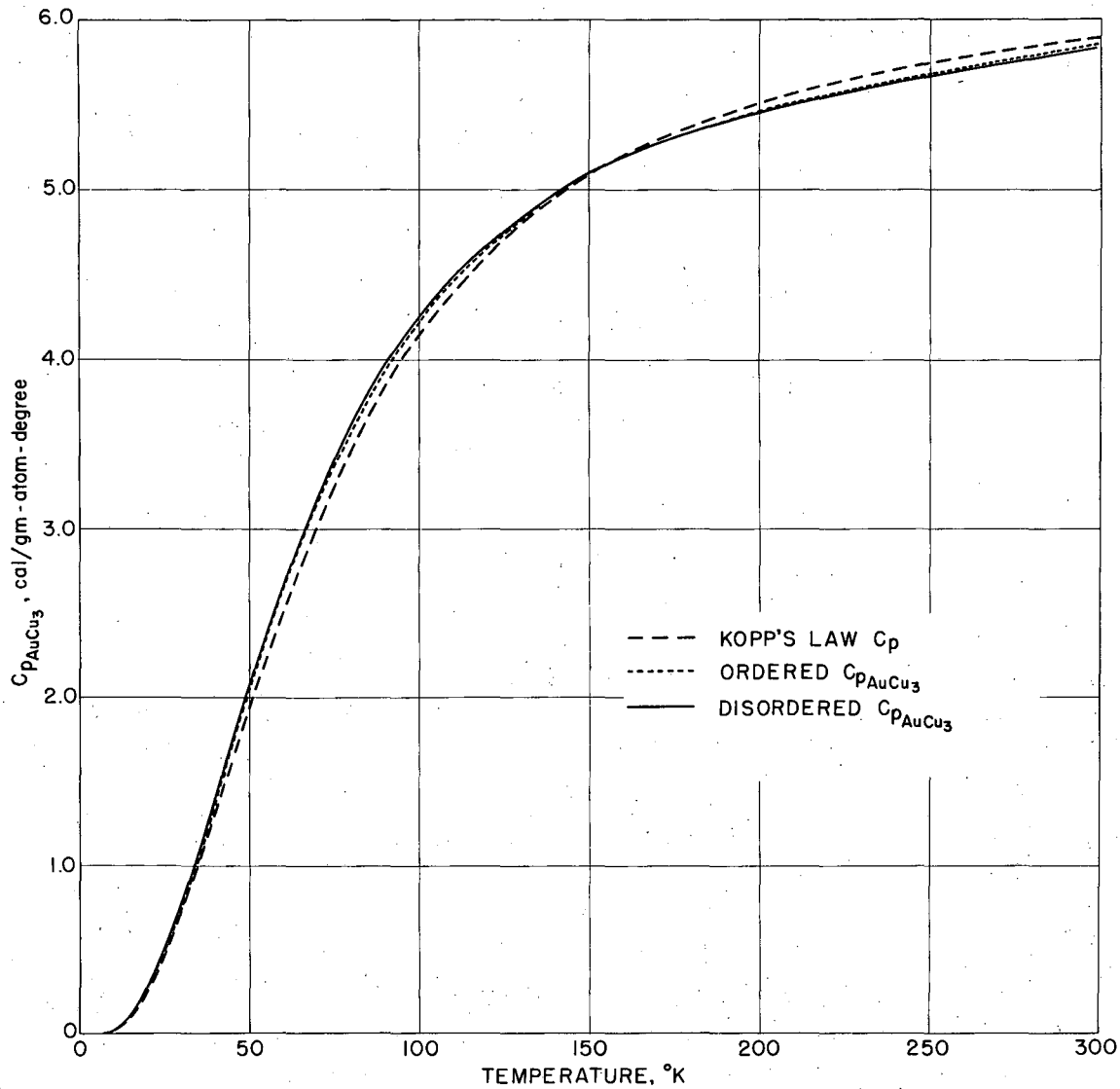

FIG. 16 HEAT CAPACITY OF ORDERED AND DISORDERED $AuCu_3$

XBL 716-6911

obtained $\Delta H_{f,\,720°K}$ = -1051 cal/g-atom for the equilibrium (completely disordered), -1180 cal/g-atom for his quenched alloy, and -1700 cal/g-atom for the ordered alloy. The result for the sample used in this study is very close to Orr's quenched sample and is only about 100 cal/g-atom more exothermic than the equilibrium sample, indicating that the sample is highly disordered.

The ΔH_f values versus temperature from the selected values of Hultgren et al.[1] shows a constant value up to 500°K, above this it starts to increase continuously, then there is a first order transformation at 663°K, following which it increases a little up to 800°K due to the destruction of short-range order. The zero point entropy (ΔS_0) of disordered $AuCu_3$ can be caculated from the high temperature data. The heat of formation and emf measurements at 800°K were combined to yield $\Delta S_{800°K}$ = 1.145 eu. Calculation of the $\Delta S_{800°K}$ using the equilibrium data as shown in Table 11 gives 1.107 eu. Using the average value of these two, 1.126 eu, and assuming that the disordered alloy obeys Kopp's law from 800°K to 298°K one can calculate ΔS_0 as shown in Table 12. A small negative correction (-0.006 eu) was applied to the calculation of ΔS to account for the fact that Kopp's law is obeyed at 400°K. The final calculation shows ΔS_0 = 0.981, while

TABLE XI. Calculation of $\Delta S^\circ_{800^\circ K}$ for Disordered $AuCu_3$ Using Heat of Formation Data

(1)	$0.25Au(0^\circ) + 0.75Cu(0^\circ) = Au_{0.25}Cu_{0.75}(0^\circ, \text{ordered})$	ΔS°_0	= 0.000 eu
(2)	$Au_{0.25}Cu_{0.75}(0^\circ, \text{ordered}) = Au_{0.25}Cu_{0.75}(298^\circ, \text{ordered})$	$(S^\circ_{298^\circ}-S^\circ_0)$	= 8.880 eu
(3)	$Au_{0.25}Cu_{0.75}(298^\circ, \text{ordered}) = Au_{0.25}Cu_{0.75}(663^\circ, \text{ordered})$	$(S^\circ_{663^\circ}-S^\circ_{298^\circ})$	= 5.354 eu
(4)	$Au_{0.25}Cu_{0.75}(663^\circ, \text{ordered}) = Au_{0.25}Cu_{0.75}(663^\circ, \text{disordered})$	ΔS°	= 0.431 eu
(5)	$Au_{0.25}Cu_{0.75}(663^\circ, \text{disordered}) = Au_{0.25}Cu_{0.75}(800^\circ, \text{disordered})$	$(S^\circ_{800^\circ}-S^\circ_{663^\circ})$	= 1.347 eu
(6)	$0.25Au(800^\circ) = 0.25Au(0^\circ)$	$-0.25(S^\circ_{800^\circ}-S^\circ_0)$	= -4.384 eu
(7)	$0.75Cu(800^\circ) = 0.75Cu(0^\circ)$	$-0.75(S^\circ_{800^\circ}-S^\circ_0)$	= 10.521 eu
	$0.25Au(800^\circ) + 0.75Cu(800^\circ) = Au_{0.25}Cu_{0.75}(800^\circ, \text{disordered})$	$\Delta S^\circ_{800^\circ}$	= 1.107 eu

TABLE XII. Calculation of ΔS°_0 for Disordered $AuCu_3$

(1)	$0.25Au(298^\circ) + 0.75Cu(298^\circ) = Au_{0.25}Cu_{0.75}(298^\circ, \text{disordered})$	$\Delta S^\circ =$	1.126 eu
(2)	$Au_{0.25}Cu_{0.75}(298^\circ, \text{disordered}) = Au_{0.25}Cu_{0.75}(0^\circ, \text{disordered})$	$-(S^\circ_{298}-S^\circ_0)\text{disord.} =$	-8.945 eu
(3)	$0.25Au(0^\circ) = 0.25Au(298^\circ)$	$0.25(S^\circ_{298}-S^\circ_0)Au =$	2.838 eu
(4)	$0.75Cu(0^\circ) = 0.75Cu(298^\circ)$	$0.75(S^\circ_{298}-S^\circ_0)Cu =$	5.962 eu
(5)	Correction to disordered $AuCu_3$ from the Kopp's Law assumption between 298° and 370°K	$\Delta S^\circ =$	-0.006 eu

$0.25Au(0^\circ) + 0.75Cu(0^\circ) = Au_{0.25}Cu_{0.75}(0^\circ, \text{disordered})$ $\quad \Delta S^\circ_0 =$ 0.981 eu

the ideal value for complete disorder is 1.117 eu. Combining this result with the heat capacity measurements in both ordered and disordered states of this alloy, one could also calculate the entropy of disordering at 298°K:

$AuCu_3$(ordered) = $AuCu_3$(disordered) $\quad \Delta S_{298} = 1.040$ eu.

IV. DISCUSSION AND CONCLUSION

Experiments by Rayne and Martin on the $AuCu_3$ alloy at liquid helium temperatures show substantially no change in electronic heat capacities on ordering, but their results show that ordering increases the Debye temperature of the lattice heat capacity by 7° according to Rayne and by 16° according to Martin, suggesting a small but definite effect on lattice heat capacity by ordering.

One would expect that the disordered state has looser bonds and some irregular lattice arrangements which give low frequency vibrations, therefore lowering the Debye temperature and raising the heat capacity of the disordered alloy at low temperatures. The specific heat of an oscillator of frequency w is given by $C_v = k(Z/\sin h Z)^2$, where $Z = \hbar w/2kT$. In an assembly of oscillators of different frequencies, all oscillators contribute the same amount to the heat capacities when temperature is high, but when T is low, only the oscillators of low frequencies make important contributions to the heat capacity.

The results of the study (shown in Fig. 17 as the difference of the heat capacity between the two states) shows C_p of the disordered state is slightly higher than that of the ordered state up to 130°K with maximum deviation of 0.07 cal/g-atom-deg.

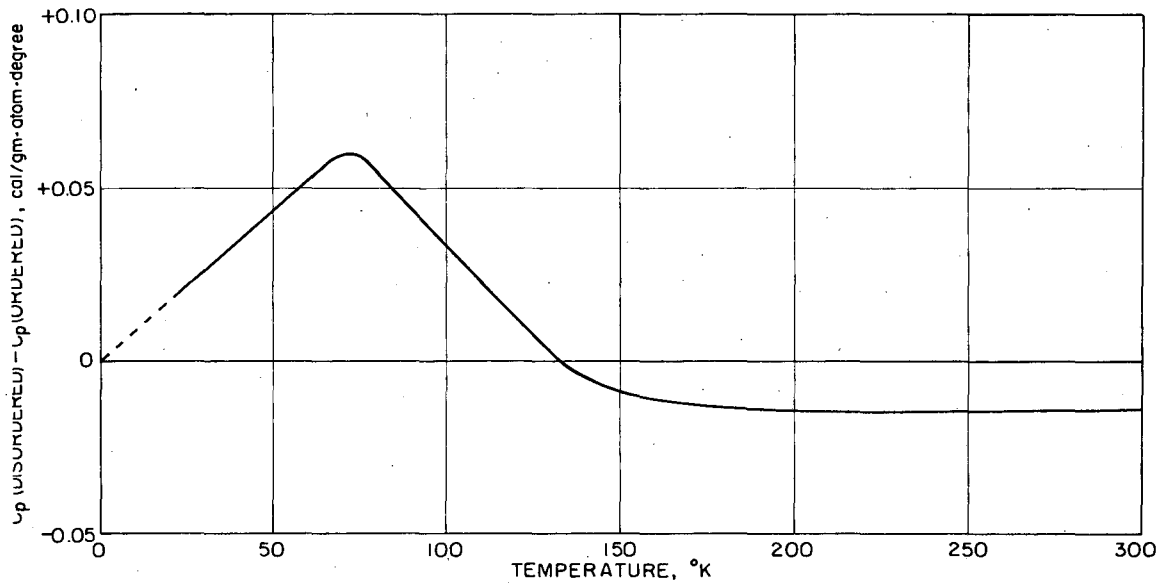

FIG. 17 HEAT CAPACITY DIFFERENCE BETWEEN THE TWO STATES OF $AuCu_3$

XBL716-6913

coming at 75°K, while above this temperature the C_p of the ordered state is higher by a small amount. This C_p difference between the two states cannot be due to systematic errors. Calculation of the apparent Debye temperature between 20°-25°K shows the following values:

$$\theta_D(\text{ordered}) = 243 \pm 2°K$$

$$\theta_D(\text{disordered}) = 239 \pm 2°K$$

Here the dilation contribution to C_p was ignored in the absence of the data needed to calculate $C_p - C_v$. These values are lower than those by Rayne and Martin, who have obtained the Debye temperature at low temperatures where the electronic term is believed to change linearly with temperature and the dilation term to be almost zero. However, θ_D of the ordered state is slightly higher than that of the disordered state, as expected.

To get the absolute heat capacity many terms should be considered. As there are no magnetic transformations nor any other phase changes in the pertinent temperature range of the study on this alloy, electronic heat capacity and dilation terms are the ones to be considered. Martin's and Rayne's result gave the coefficients of electronic heat capacities (γ) of the ordered and disordered states as 1.65×10^{-4} and 1.58×10^{-4}, respectively. As these electronic heat capacities are small at the

temperatures of the study, the differences in electronic heat capacities does not affect the difference of the lattice heat capacities of the two states.

The dilation term may be obtained with the aid of the thermodynamic relationship:

$$C_p - C_v = 9\alpha^2 VT/\chi$$

where χ = compressibility

α = expansion coefficient

V = atomic volume

While these data are not available, one could approximate the term using the Nernst-Lindeman approximation,[36] $C_p - C_v = 0.0214 C_p^2 (T/T_m)$ where T_m is the melting point of the alloy, 1250°K for $AuCu_3$. The calculation on this base gives an idea of the magnitude of this term. They were found to be 0.00003 and 0.17 cal/g-atom-deg at 25° and 300°K, respectively. This shows that at low temperatures the dilation term is negligible but it becomes significant at higher temperatures. The exact calculation of the dilation term is not possible because of the lack of data, however, if the dilation term of the ordered state is higher than that of the disordered state, this could account for the fact that the ordered state has the higher C_p above 130°K although its vibrational C_p, as determined at

lower temperatures, is smaller.

The value of the zero point entropy for idsordered $AuCu_3$, 0.981 eu, is near the ideal value for complete disorder of 1.117 eu for this composition. That it is somewhat lower than the theoretical value was confirmed by the heat of formation measurements, which show that the sample had a small amount of short-range order. This could not be detected on the x-ray pattern.

ACKNOWLEDGEMENTS

I wish to express my deep appreciation to:

My wife, Anne Ja, who gave encouragement and patience.

Professor Ralph Hultgren, who has given continued guidance and support throughout my graduate career.

Dr. Donald T. Hawkins, who has been of much help to me in many discussions about the calorimeter.

Mr. Stanley E. Ross, who devoted many hours in assisting with the experimental work.

Mr. Eugene H. Huffman, who analyzed the chemical composition of the Mg_3Sb_2 alloy.

Mrs. Rebecca Palmer, who typed the manuscript.

Mrs. Gloria Pelatowski, who prepared the drawings.

This work was performed under the auspices of the U.S. Atomic Energy Commission.

REFERENCES

1. Hultgren, R., R. L. Orr, P. D. Anderson, and K. K. Kelley (1963) Selected Values of Thermodynamic Properties of Metals and Alloys, John Wiley and Sons Inc., New York.
2. Hultgren, R., R. L. Orr, and K. K. Kelley (1964 to date) Supplement to Selected Values of Thermodynamic Properties of Metals and Alloys. (Loose-leaf sheets issued at irregular intervals.)
3. Anderson, P. D. (1966) Ph. D. Thesis, University of California, Berkeley.
4. Swalin, R. A. (1967) Thermodynamics of Solids, John Wiley and Sons Inc., New York.
5. Cottrell, A. H. (1960) Theoretical Structural Metallurgy, St. Martin's Press Inc., New York.
6. Piesbergen, U. (1963) Z. Naturforsch. 18a, 141.
7. Ohmura, Y. (1965) J. Phys. Soc. 20, 350.
8. Jelinek, F. J., W. D Shickell, and B.C. Gerstein (1966) J. Phys. Chem. Solids, 28, 267.
9. Martin, D. L. (1960) Can. J. Phys. 38, 25.
10. Satterthwaite, C. B., R. S. Craig, and W. E. Wallace (1954) J. Am. Chem. Soc. 76, 232.

11. Coffer, L. W., R. S. Craig, C. A. Kreir, and W. E. Wallace (1954) J. Am. Chem. Soc. 76, 241.

12. Hawkins, D. T., and R. Hultgren (1971) J. Chem. Thermodynamics 3, 175.

13. Huffstutler, M. C., Jr. (1961) Ph. D. Thesis, University of California, Berkeley.

14. Yoon, H. (1968) M. S. Thesis, University of California, Berkeley.

15. Heumann, T., and B. Predel (1966) Z. Metallk., Bd. 57, 50.

16. Pearson, W. B. (1958) A Handbook of Lattice Spacing and Structures of Metals and Alloys, Pergamon Press, New York.

17. Hansen, M., and K. Anderko (1958) Constitution of Binary Alloys, McGraw-Hill, New York.

18. Kleppa, O. J. (1956) J. Phys. Chem. 60, 858.

19. Kubaschewski, O. (1943) Z. Physik. Chem. 192, 292.

20. Kubaschewski, O., and A. Walter (1939) Z. Elektrochem. 45, 732.

21. Kubaschewski, O., and J. A. Catterall (1956) Thermodynamic Data of Alloys, Pergamon Press, London.

22. Eueken, A. (1909) Physik. Z. 10, 586.

23. Nernst, W. (1910) Chem. Abstracts, 4, 2397.

24. Giauque, W. F., and C. J. Egan (1937) J. Chem. Phys. 5, 45.

25. Gibson, G. E., and W. F. Giauque (1923) J. Am. Chem. Soc. 45, 93.

26. Hawkins, D. T. (1970) Ph. D. Thesis, University of California, Berkeley.

27. Kelley, K. K., and G. E. Moore (1943) J. Am. Chem. Soc. 65, 2340.

28. Shomate, C. H. (1945) J. Chem. Phys. 31, 326.

29. Born, M., and Th. Von Karman (1912) Physikal Ztschr. 13, 297.

30. Kelley, K. K., and E. G. King (1961) Contribution to the Data on Theroretical Metallurgy, Bulletin 592, Bureau of Mines, Washington.

31. Rayne, J. A. (1957) Phys. Rev. 108, 649.

32. Martin, D. L. (1968) Can. J. Phys. 49, 923.

33. Flinn, P. A., G. M. McManus, and J. A. Rayne (1960) J. Phys. Chem. Solids 15, 189.

34. Rosenstock, H. B. (1962) J. Phys. Chem. Solids, Pergamon Press 23, 659.

35. Anderson, O. L. (1959) J. Phys. Chem. Solids 12, 41.

36. Lasjaunias, J. C. (1969) C. R. Acad. Sc. Paris, t. 269.

37. Orr, R. L (1960) Acta Metallurgica 8, 489.

38. Nernst, W., and F. Lindemann (1911) Z. Elektrochem. 17, 817.

TECHNICAL INFORMATION DIVISION
LAWRENCE BERKELEY LABORATORY
UNIVERSITY OF CALIFORNIA
BERKELEY, CALIFORNIA 94720